

3.12 Comparison of Test vs Analysis

Physical testing of the ES-3100 shipping container to the 4-foot, 30-foot, 30-foot crush and 40-inch punch impacts were carried out in late May, 2004 at the Oak Ridge National Lab (ORNL), National Transportation Research Center (NTRC) facility in Oak Ridge.

The test specimen were subject to the entire series of impacts (4-foot, 30-foot, crush and punch), however the analytical impacts were not all subject to the entire series. Typically, the analysis was a design run which was subjected to a 30-foot impact followed by a crush impact. So the 30-foot analysis comparison was made to a test specimen that had experienced a 4-foot and a 30-foot impact. And likewise for the crush impact comparisons, the analysis results are lacking the initial 4-foot impact.

The comparisons are made for TU1 (Test Unit #1), TU2, TU3 and TU4. TU1 is the 12° slakedown, TU2 is the cold package side impact, TU3 is the corner impact and TU4 is the end impact. The nodes in the analysis model shell elements lie on the thickness centerline. Therefore, where appropriate, half thickness dimensions are included to render surface to surface comparisons with the test data. Figure 3.12.1 shows locations for which test diameters were obtained.

Dimensions in the tables are inches, unless otherwise noted. The analysis model was reflected with the post processor so that it appears as a full model. This was done to aid in the visual comparison between the test specimen and the model results. The background in the test photos has been erased, also to aid visual comparisons.

The "flats" is the region of relative flatness in the drum liner due to the impact. The analysis flats dimensions are obtained by knowing the element width (whole widths used) and judging which elements are dominantly in a relatively flat plane. The test flat dimensions are taken by visually judging when the drum deviates from a permanent, relatively flat region.

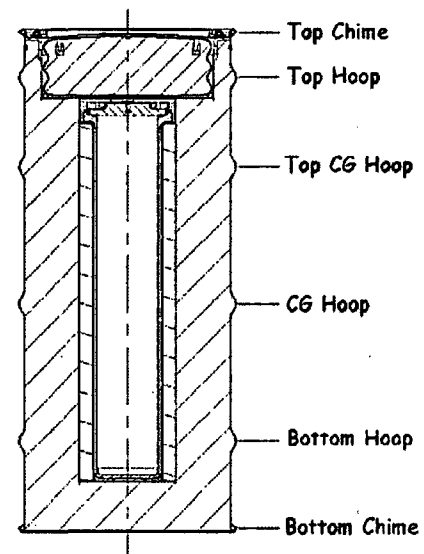


Figure 3.12.1 - Locations of Test Diameter Measurements

3.12.1 Comparison of Run4g to TU1

Run4g is a 30-foot, 12° slapdown impact followed by an offset crush (crush plate centered over the CV flange). TU1 is a 12° slapdown with a 4-foot impact, 30-foot impact, offset crush, and punch test specimen. The following Table 3.12.1.1 shows the initial diameter comparisons (pre-impact) using test data compared to the analysis results.

Location	0° - 180°		90° - 270°	
	Test	Analysis	Test	Analysis
Top Chime	19.25	19.32	19.25	19.32
Top Hoop	19.25	19.37	19.25	19.37
Top CG Hoop	19.25	19.37	19.25	19.37
CG Hoop	19.25	19.37	19.25	19.37
Bottom Hoop	19.25	19.37	19.25	19.37
Bottom Chime	19.25	19.38	19.25	19.38

The Table 3.12.1.2 shows the digital results of the 30-foot impact. The test diameters are after the 4 and 30-foot impacts, while the analysis is after the 30-foot impact.

	0° - 180°		90° - 270°	
	Test	Analysis	Test	Analysis
Top Chime	18-1/2	18.1	19-3/8	19.5
Top Hoop	18-1/2	18.2	19-3/8	19.6
Top CG Hoop	18-1/2	18.5	19-3/8	19.5
CG Hoop	18-5/8	18.8	19-3/8	19.4
Bottom Hoop	18-5/8	18.9	19-1/4	19.3
Bottom Chime	17-13/16	18.1	19-3/8	19.4

Figure 3.12.1.1 shows the final configuration of the test specimen after the 4 and 30-foot impacts. Figure 3.12.1.2 shows the analytical model configuration after the 30-foot impact.



Figure 3.12.1.1 - TU1, Results of 30-Foot Impact

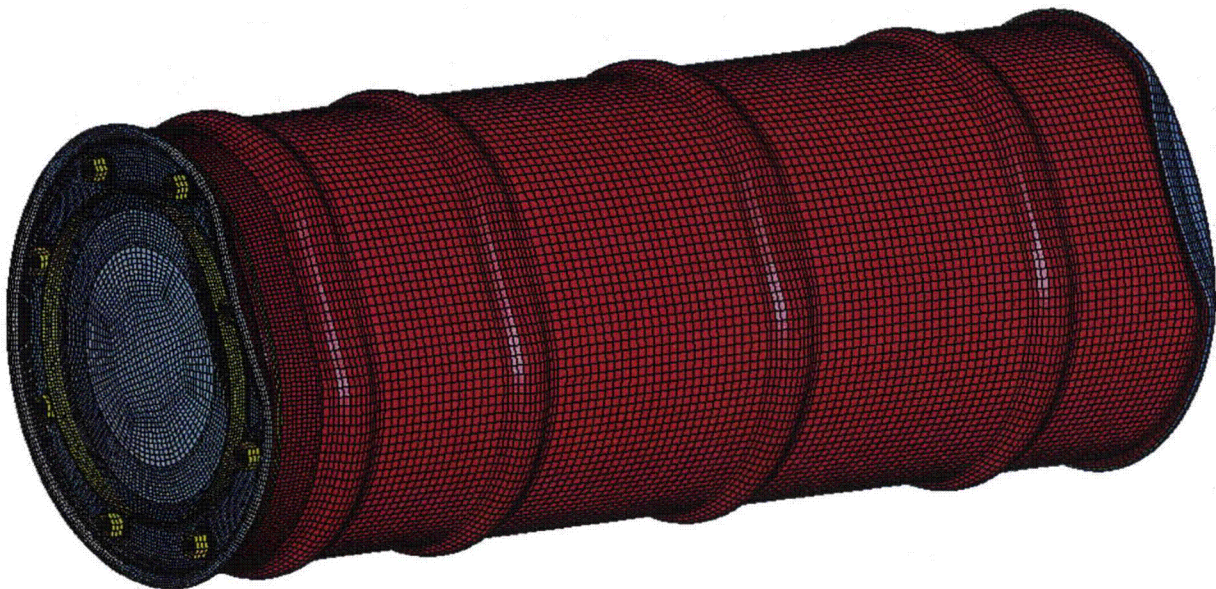


Figure 3.12.1.2 - Run4g, Results of the 30-Foot Impact

Table 3.12.1.3 shows the comparison of the digital results of the crush impact. The test data is for the cumulative effects of a 4-foot, 30-foot, and crush impact. The analysis data is for a cumulative 30-foot impact and crush impact.

Table 3.12.1.3 - Run4g vs TU1, Diameter Results After the Crush Impact				
	0°-180°		90°-270°	
	Test	Analysis	Test	Analysis
Top Chime	15-5/8	15.0	20-5/8	20.7
Top Hoop	16	15.3	20-7/16	20.8
Top CG Hoop	16-1/4	15.9	20-1/4	20.6
CG Hoop	16-1/2	16.4	19-7/8	20.1
Bottom Hoop	18-1/4	18.3	19-1/2	19.6
Bottom Chime	17-13/16	18.1	19-1/4	19.4

Figure 3.12.1.3 shows an isometric view of the test specimen with the crush side up. Figure 3.12.1.4 shows a similar view for the analysis results.



Figure 3.12.1.3 - TU1, View of Crush Damage with the Crush Side Up



Figure 3.12.1.4 - Run4g, View of the Crush Damage With the Crush Side Up

Table 3.12.1.4 shows the results of a comparison of the "flats" measurements on the drum for the 30-foot impact and Table 3.12.1.5 compares the crush impact test measurements and analysis results.

	Test	Analysis
Top Chime	8	8.8
Top Hoop	7-3/8	8.4
Top CG Hoop	7-1/8	7.6
CG Hoop	6-3/8	5.9
Bottom Hoop	6-3/4	5.9
Bottom Chime	10	10.1

Location	Rigid Surface Side		Crush Plate Side	
	Test	Analysis	Test	Analysis
Top Chime	9	10.5	8-1/2	10.5
Top Hoop	10	11.0	10	11.0
Top CG Hoop	10	10.1	10-1/8	10.1
CG Hoop	9	8.4	10-5/8	10.1
Bottom Hoop	8-1/4	7.6	---	0.0
Bottom Chime	9-7/8	10.1	---	0.0

The stud at the 90° position was severed in the model (reference Section 3.7, Figure 3.7.6), however arguments were made that the lid would tear first, relieving the loading on the stud. This was verified in the test results where tears were noted at both stud holes at 90° to the impacts/crush.

3.12.2 Comparison of Run2e vs TU3

Run2e is a CG over lid corner 30-foot impact, followed by a bottom corner crush. TU3 is a similar impact configuration with a 4-foot impact and 30-foot impact on the lid corner, then a crush impact on the bottom corner followed by a punch.

Test measurements show that there is 1.125 inches between the top chime and the top hoop in the test. Similar measurements in the analysis show that the distance is about 1.7 inches. This would be a somewhat judgmental comparison due to points chosen for measurement on the test specimen might not be the same as those chosen in the analysis. The analysis measurement is from the top of the crimped drum roll to the center of the flattened region in the lid roll, on the plane of symmetry. Actual point locations chosen in the test measurements are not known.

Table 3.12.2.1 shows the comparison of the TU3 test unit and the computer run2e diameter changes after the 30-foot impact.

	0°-180°		90°-270°	
	Test	Analysis	Test	Analysis
Top Chime	19-1/4	19.0	19-3/16	19.1
Top Hoop	18-5/8	19.1	19-7/8	20.0
Top CG Hoop	19-1/8	19.4	19-3/8	19.5
CG Hoop	19-1/8	19.4	19-3/8	19.4
Bottom Hoop	19-1/8	19.4	19-1/4	19.4
Bottom Chime	19-1/8	19.3	19-3/8	19.4

Figure 3.12.2.1 is an image of the damage after the 30-foot impact of TU3. The test photo shows the cumulative damage from the 4-foot and 30-foot impacts. Figure 3.12.2.2 shows the analysis damage from only the 30-foot impact.

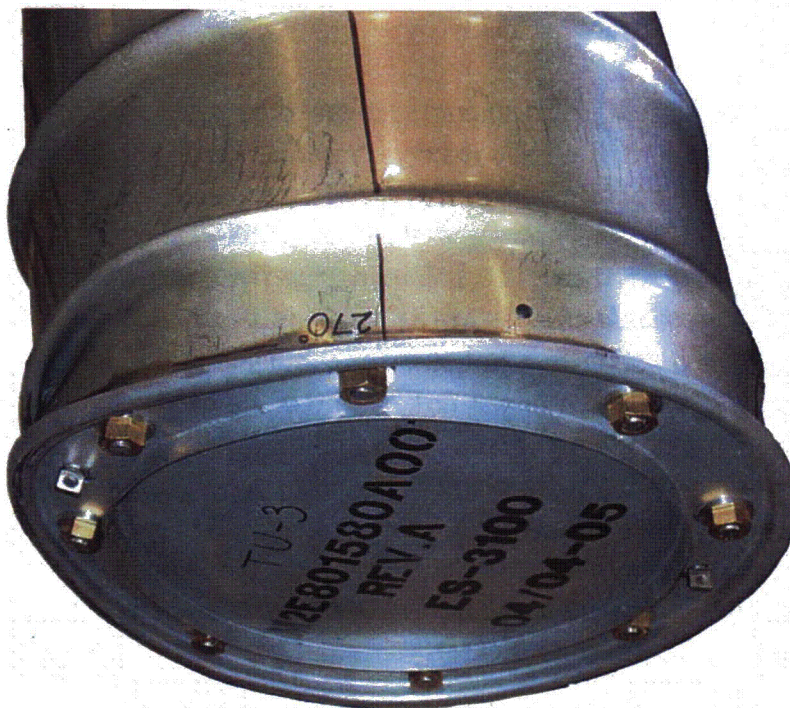


Figure 3.12.2.1 - TU3, Deformed Shape After the 30-Foot Impact

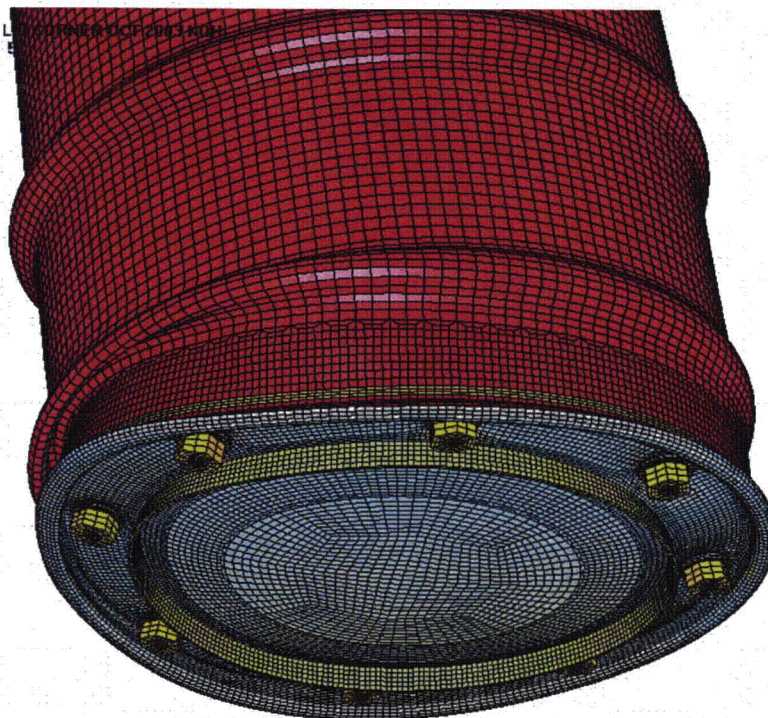


Figure 3.12.2.2 - Run2e, Deformed Shape After the 30-Foot Impact

The package diameters after the crush impact are compared in Table 3.12.2.2.

Table 3.12.2.2 - Run2e vs TU3, Diameter Results After the Crush Impact				
	0°-180°		90°-270°	
	Test	Analysis	Test	Analysis
Top Chime	19-1/4	19.0	19-1/16	19.0
Top Hoop	18-3/4	18.9	20-1/4	20.6
Top CG Hoop	19-1/4	19.4	19-3/4	19.9
CG Hoop	19-1/8	19.3	19-1/4	19.4
Bottom Hoop	19-1/8	19.3	19-3/4	20.4
Bottom Chime	18	18.6	19-3/8	19.4

The final images after the crush impact are shown for the test and the analysis. Figure 3.12.2.3 shows the final shape of the crushed bottom on the test specimen (4ft + 30ft + crush impacts) and Figure 3.12.2.4 shows a similar view of the analysis (30ft + crush impacts).



Figure 3.12.2.3 - TU3, Damage to the Bottom Head in the Crush Impact

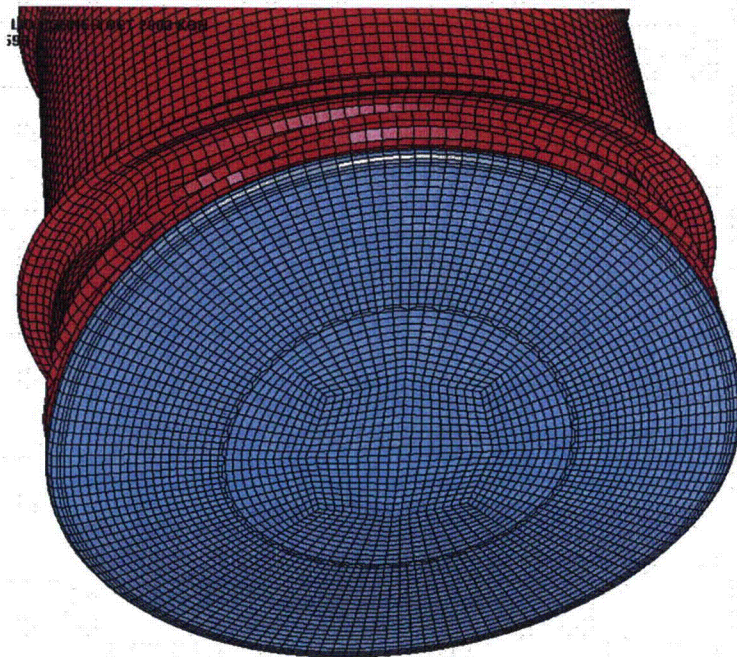


Figure 3.12.2.4 - Run2e, Damage to the Bottom Head in the Crush Impact

The damage to the lid region at the end of the crush impact is shown in Figure 3.12.2.5 for the TU3. The damage to the lid region in the analysis run2e is shown in Figure 3.12.2.6. Note that the stud at the initial 30-foot impact onto the rigid surface has failed in the test. Elevated plastic strains throughout the stud shank are noted in Section 3.5 along with discussion about the stud.



Figure 3.12.2.5 - TU3, Lid Damage from the Crush Impact

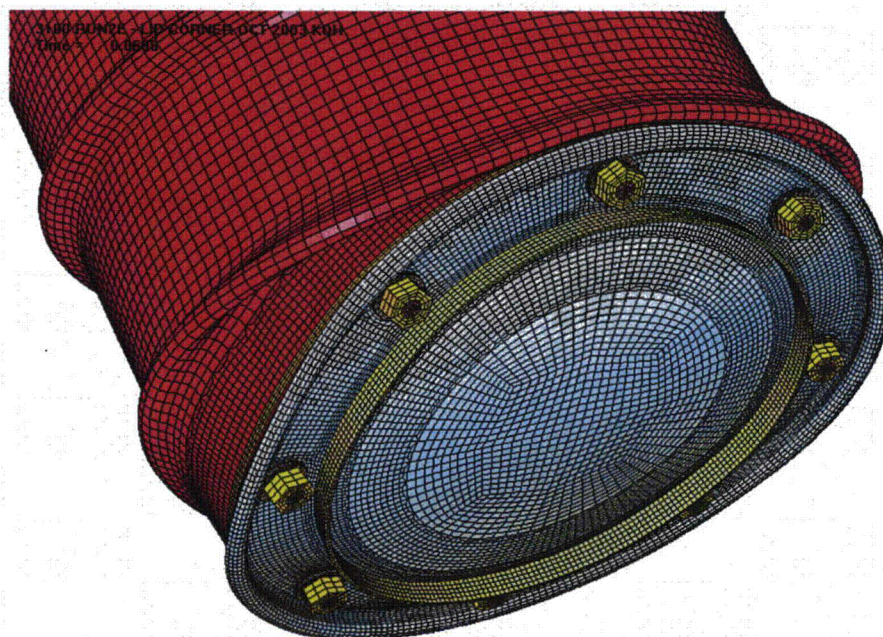


Figure 3.12.2.6 - Run2e, Lid Damage from the Crush Impact

3.12.3 Comparison of Run3b vs TU4

The run3b is a 30-foot lid end down impact onto the rigid surface, followed by a crush impact onto the container bottom. TU4 is a test unit subjected to a 4- and 30-foot impact onto the lid end, followed by a crush impact onto the bottom.

The diameter measurements after the 30-foot impact are given in Table 3.12.3.1.

	0°-180°		90°-270°	
	Test	Analysis	Test	Analysis
Top Chime	19-1/4	19.3	19-3/8	19.3
Top Hoop	19-1/8	19.7	19-7/8	19.7
Top CG Hoop	19-13/16	20.0	19-3/8	20.0
CG Hoop	19-1/8	19.5	19-1/4	19.5
Bottom Hoop	19-1/4	19.4	19-1/4	19.4
Bottom Chime	19-1/4	19.4	19-1/4	19.4

The overall height measurements of the drum are compared. The 30-foot impact test results vary around the circumference: 43.0 inches at 0°, 43.125 inches at 90°, 42.875 inches at 180° and 42.625 inches at 270°. The analysis is symmetrical, and the height from the top of the lid drum roll to the bottom head surface after the 30-foot impact is about 42.6 inches.

Figure 3.12.3.1 shows the configuration of the TU4 after the 30-foot impact (4ft + 30ft). Figure 3.12.3.2 shows the analysis model configuration after the 30-foot impact in a similar orientation to the test unit.



Figure 3.12.3.1 - TU4, 30-Foot Impact Damage

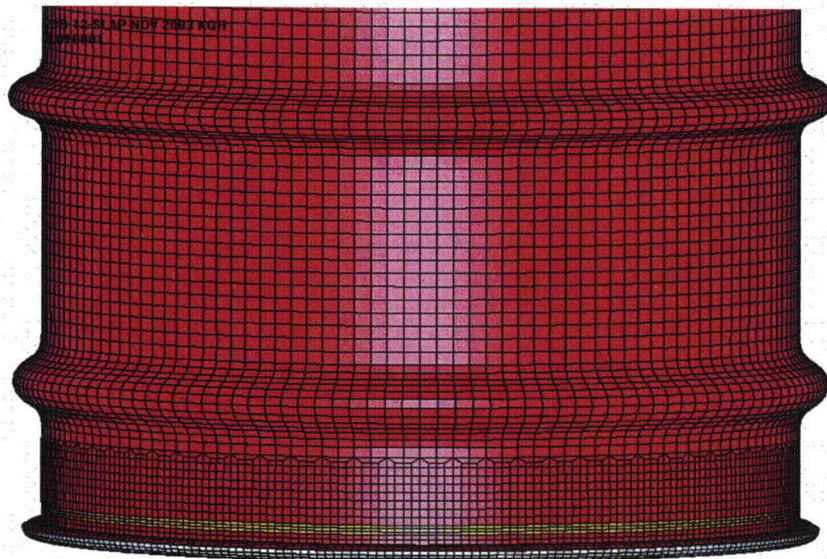


Figure 3.12.3.2 - Run3b, 30-Foot Impact

The height measurement of TU4 after the crush impact is 39.375 inches at 0°, 40.375 inches at 90°, 40.625 inches at 180°, and 39.75 inches at 270°. The analytical value for the height is about 38.9 inches.

The diameters after the crush impact are compared in Table 3.12.3.2.

	0°-180°		90°-270°	
	Test	Analysis	Test	Analysis
Top Chime	19-1/4	19.3	19-3/8	19.3
Top Hoop	20	20.2	20-1/8	20.2
Top CG Hoop	20	20.2	20-1/16	20.2
CG Hoop	19-7/16	20.1	19-1/2	20.1
Bottom Hoop	19-15/16	20.5	20	20.5
Bottom Chime	19-1/4	19.4	19-1/4	19.4

Figure 3.12.3.3 shows the TU4 at the end of the crush impact (4ft + 30ft + crush), while Figure 3.12.3.4 shows the configuration of the run3b model (30ft + crush).

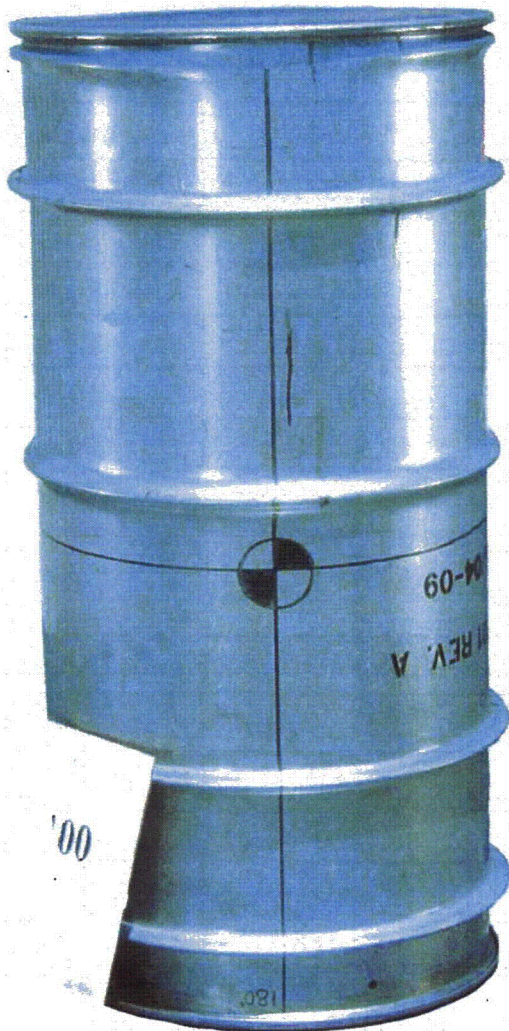


Figure 3.12.3.3 - TU4, Crush Damage



Figure 3.12.3.4 - Run3b, Crush Damage

3.12.4 Comparison of Run1hh vs TU2

Run1hh was the upper bounding kaolite (-40°F) run which included a 4-ft, 30-foot, crush, and punch impacts. The test results are for the cumulative damage from all four impacts, therefore, only one set of data is compared. The table 3.12.4.1 shows the results for the diameter changes due to all four impacts for the test and the analysis.

	0°-180°		90°-270°	
	Test	Analysis	Test	Analysis
Top Chime	17-5/8	18.1	19-13/16	19.5
Top Hoop	17-3/8	16.7	19-3/4	20.0
Top CG Hoop	17	16.5	20	20.3
CG Hoop	16	16.4	20-1/4	20.4
Bottom Hoop	15-1/2	16.3	20-1/8	19.9
Bottom Chime	18	17.7	19-3/8	19.4

Table 3.12.4.2 shows the comparison of the "flats" dimensions for the test and the analysis.

	180° - Crush Plate Side		0° - Rigid Surface Side	
	Test [‡]	Analysis	Test	Analysis
Top Chime	6-1/4	0	8.0	9.2
Top Hoop	8-7/8	10.1	9.0	8.4
Top CG Hoop	9-5/8	8.4	10-1/8	8.4
CG Hoop	12	9.3	9-7/8	9.3
Bottom Hoop	14-7/8	10.1	9-7/8	9.3
Bottom Chime	0	0	9-3/8	10.1

‡ - Note - The crush plate edge was 4.75 inches from bottom of package, therefore the top chime was engaged with the crush plate in the test.

A visual comparison of the cumulative damage on the rigid surface side after the four impacts is shown in Figures 3.12.4.1 (test) and Figure 3.12.4.2 (analysis).



Figure 3.12.4.1 - TU2, Cumulative Damage After the Punch Impact, Rigid Surface Side



Figure 3.12.4.2 - Run1hh, Cumulative Damage After the Punch Impact, Rigid Surface Side

A visual comparison of the cumulative damage on the crush side after the four impacts is shown in Figures 3.12.4.3 (test) and Figures 3.12.4.4 (analysis).

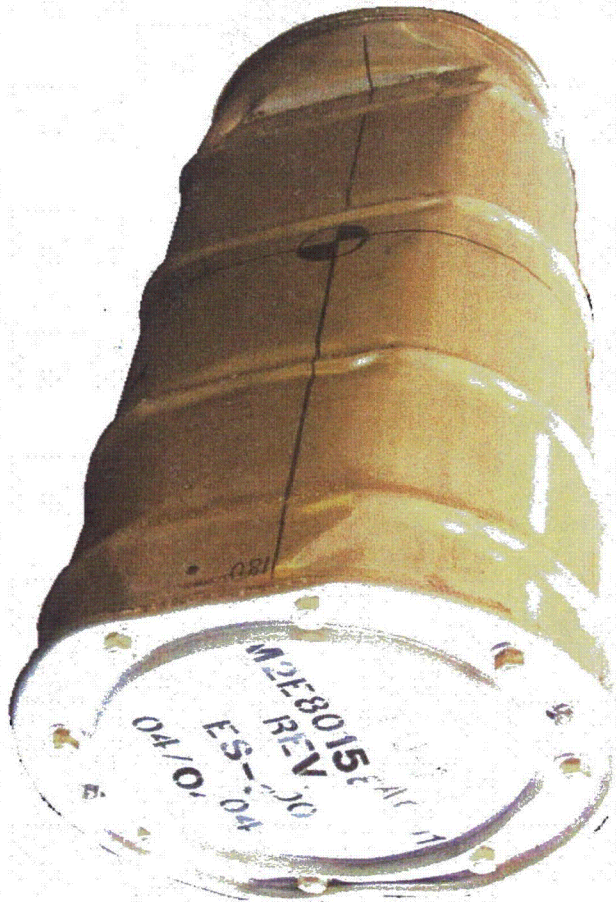


Figure 3.12.4.3 - TU2, Cumulative Damage After the Punch Impact, Crush Plate Side



Figure 3.12.4.4 - Run1hh, Cumulative Damage After the Punch Impact, Crush Plate Side

4.0 Summary and Conclusions

The response of the ES-3100 shipping container to various 10CFR71 required impacts is presented in Sections 3.1 to 3.10. The maximum effective plastic strain for each component in the Section 3.1 to 3.10 impacts is summarized in Table 4.0.1. The effective plastic strain for shell elements in Table 4.0.1 is maximum surface strain. Section 3.11 presents the response of the drum to various punch angles. The maximum effective plastic strain for the drum in each punch angle orientation of Section 3.11 is summarized in Table 4.0.2. Section 3.12 compares the analytical results to physical test results.

Maximum strains in excess of 0.5 in/in are near the 304L strain limit of 0.57 in/in and are highlighted in red in Table 4.0.1. The components which are highlighted include the drum, lid, studs and liner.

From Table 4.0.1, the fact that is apparent is the high demand placed on the drum lid and studs. During the design phase of the ES-3100, an effort was made to minimize the number of fasteners in the drum lid. The relatively high lid/stud strains are therefore a precipitate of that effort. The side and slapdown impacts place a high demand on the lid/stud components.

In the side crushes (run1g, run1ga, run1hl, run1hh, run4g, run4ga, run4h and run4ha) a large demand is placed on the lid and the studs. In all the runs the impact of concern is the crush impact and the demand it places on the lid and studs. In all the runs, the relatively high levels of effective plastic strain (surface and membrane) are shown to exist over localized regions of stud/lid interaction in the lid. Investigations revealed that the elevated plastic strains in the lid occurred before the studs experienced elevated strain levels. Therefore, it would be expected that the lid would tear and relieve loading on the studs, before the studs would fail. Some tearing of the lid may take place, but catastrophic tearing or ripping of the lid is not predicted. The large washer would restrain the lid, even if the crimping of the lid/drum roll didn't pin the lid in place. This was verified in the TU1 test specimen with local tearing at the stud holes at 90° and 270° without the loss of a stud.

Table 4.0.1 - ES-3100 Shipping Package Summary of Component Maximum Effective Plastic Strains (in/in)

Material	Description	Run1g		Run1ga		Run1hl				Run1hh			
		Side (Section 3.1)		Side (Section 3.2)		Side - Lower Bound Kaolite (Section 3.3)				Side - Upper Bound Kaolite (Section 3.4)			
		Impact	Centered Crush	Impact	Offset Crush	4-foot	30-foot	Centered Crush	Punch	4-foot	30-foot	Centered Crush	Punch
1	CV Body	0.0346	0.0348	Same as Run1g Impact Results	0.0348	0.0263	0.0287	0.0287	0.0299	0.0298	0.0386	0.0462	0.0599
3	CV Lid	0.0002	0.0002		0.0002	0.0000	0.0001	0.0003	0.0006	0.0000	0.0000	0.0004	0.0004
4	CV Nut Ring	0.0000	0.0000		0.0000	0.0000	0.0000	0.0000	0.0000	0.0000	0.0000	0.0000	0.0000
5	Angle	0.0682	0.0945		0.1058	0.0054	0.0777	0.1178	0.1178	0.0059	0.0622	0.0816	0.0816
6	Drum	0.2218	0.3028		0.3818	0.1561	0.2250	0.5309	0.5309	0.1170	0.2259	0.2623	0.2623
7	Drum Bottom	0.2444	0.2945		0.2444	0.0991	0.2125	0.3342	0.3345	0.1215	0.2528	0.2807	0.2807
10	Liner	0.1189	0.2063		0.2853	0.0537	0.1800	0.2637	0.2637	0.0598	0.0970	0.2005	0.2027
12	Lid	0.3580	0.6430		1.1345	0.1320	0.5180	1.2969	1.2971	0.0860	0.4073	0.6411	0.6411
15	Lid Stiffener	0.0060	0.0303		0.1116	0.0001	0.0118	0.0530	0.0530	0.0000	0.0069	0.0217	0.0217
16	Lid Studs	0.1171	0.1937		0.5207	0.0000	0.1098	0.4159	0.4221	0.0000	0.1226	0.1753	0.1761
17	Lid Stud Nuts	0.0005	0.0005		0.0103	0.0000	0.0000	0.0007	0.0007	0.0000	0.0000	0.0000	0.0000
18	Lid Stud Washer	0.1628	0.1628		0.1685	0.0011	0.0225	0.0832	0.0844	0.0310	0.0951	0.1034	0.1034
19	Plug Liner	0.0826	0.1212		0.2181	0.0022	0.0956	0.1256	0.1256	0.0046	0.0995	0.1258	0.1258

Material	Description	Run2e		Run3b		Run4g		Run4ga		Run4h		Run4ha	
		Corner (Section 3.5)		End (Section 3.6)		Slapdown (Section 3.7)		Slapdown (Section 3.8)		Slapdown (Section 3.9)		Slapdown (Section 3.10)	
		Impact	Crush	Impact	Crush	Impact	Offset Crush	Impact	Centered Crush	Impact	Offset Crush	Impact	Centered Crush
1	CV Body	0.0142	0.0364	0.0012	0.0053	0.0445	0.0457	Same as Run4g Impact Results	0.0741	0.0450	0.0461	Same as Run4h Impact Results	0.0839
3	CV Lid	0.0024	0.0024	0.0031	0.0034	0.0003	0.0005		0.0006	0.0000	0.0004		0.0013
4	CV Nut Ring	0.0000	0.0000	0.0000	0.0000	0.0000	0.0000		0.0003	0.0000	0.0000		0.0000
5	Angle	0.0393	0.0464	0.0287	0.0304	0.0881	0.1045		0.0917	0.0861	0.1071		0.0881
6	Drum	0.3238	0.3787	0.0565	0.1258	0.3017	0.3972		0.3537	0.3017	0.3881		0.3848
7	Drum Bottom	0.0000	0.0731	0.0024	0.0312	0.2877	0.2877		0.2919	0.2877	0.2877		0.2922
10	Liner	0.3797	0.5507	0.1665	0.3585	0.1234	0.2702		0.2363	0.1181	0.2475		0.2633
12	Lid	0.2968	0.3579	0.1094	0.1415	0.5537	1.0797		1.0796	0.3831	0.9830		0.6336
15	Lid Stiffener	0.0271	0.0272	0.0068	0.0098	0.0232	0.0838		0.0303	0.0184	0.1083		0.0338
16	Lid Studs	0.5197	0.5578	0.0962	0.1541	0.1737	>0.57		0.3174	0.0891	0.5364		0.1705
17	Lid Stud Nuts	0.2252	0.2258	0.0162	0.0170	0.0000	0.0086		0.0000	0.0000	0.0052		0.0000
18	Lid Stud Washer	0.0907	0.1111	0.0510	0.0510	0.0597	0.1003		0.0597	0.0782	0.0885		0.0782
19	Plug Liner	0.1131	0.1170	0.0636	0.0944	0.1290	0.2715		0.1636	0.1592	0.2719		0.1832

Table 4.0.2 - ES-3100 Punch Angle Variation		
Punch Angle	Maximum Effective Plastic Strain in the Drum (in/in)	
	Surface	Membrane
0	0.2030	0.1385
10	0.1204	0.0633
20	0.1100	0.0529
30	0.1551	0.0951
40	0.1632	0.1115
50	0.3340	0.1238
60	0.1844	0.0646
63.6	0.3895	0.1858

The drum in run1hl (lower bounding kaolite impacts) is shown to experience a high demand during the centered crush impact. The regions of high effective plastic strain are in the drum at each edge of the crush plate. The lid end of the drum experiences the highest strain (about 0.53 in/in), but its magnitude is below the failure limit of 0.57 in/in in bending and less than (about 0.36 in/in) in membrane. Therefore, tearing of the drum is not expected.

The liner in run2e (corner impact) also experiences relatively high effective plastic strain in its crush impact (about 0.55 in/in). This is in a region of localized crimping and the membrane strain is found to be about 0.25 in/in. Therefore, tearing of the liner is not expected.

The run2e corner impact shows high effective plastic strain in the drum stud at the 0° position (at the initial impact point with the rigid surface). The region of high strain exists across the diameter of the stud, near its attachment to the angle. High strain levels are shown in the 30-foot impact (about 0.52 in/in) and higher in the crush impact (about 0.56 in/in). Two factors direct concern to this stud. One factor is that this stud is right at the rigid surface and, therefore, experiences direct loading between the shipping package and the rigid surface. The second factor is that effective plastic strain quickly (about 0.003 seconds into the 30-foot impact) reaches a significant value (about 0.5 in/in) throughout the stud shank. Slight changes in configuration in the stud from the modeled configuration (e.g. length, end configuration and boundary conditions) could quickly elevate the strains past failure. Boundary conditions such as changes in the friction factor could also prove detrimental for the stud. This was verified in the test

with the failure of the stud at 0°.

The CV lid/body flange separation is reported as time history nodal separation data. The data is from a transient analysis and therefore contains analytical ringing or contact chatter. The maximum gap spike value is about 0.012 inches in run3b. The largest elevated value of gap is also for run3b and is between 0.008 inches and 0.010 inches for about 0.005 seconds. The gap response is oscillatory in nature and reaches an average value of 0.003 inches or less.

In conclusion, review of the results of the ES-3100 borobond design runs presented in this calculation predict:

- 1) The lid is predicted to locally tear at the stud holes in the side and slapdown crush impacts. Extensive tearing is not predicted. The studs are predicted to remain in place to secure the lid in the side and slapdown impacts.
- 2) The single stud at the point of contact in the corner impact could easily fail. The remainder of the studs in the corner impact experience relatively low demand and are predicted to restrain the lid/plug. The failure of the single stud, would not result in shielding or thermal protection concerns for the CV.
- 3) The maximum CV lid/body flange separation spikes to about 0.012 inches briefly, and between 0.008 to 0.010 inches for about 0.005 seconds. The maximum relaxed value of the gap would be expected to be 0.003 inches or less.
- 4) The remaining kaolite thickness is shown in time history plots in each analysis results in summarized in Section 3(e.g., Figure 3.1.33).

5.0 References

- 5.1 The software "TrueGrid", by XYZ Scientific Applications, Inc, Version 2.1.5.
- 5.2 Livermore Software Technology Corporation (LSTC), "LS-Dyna", A Program for Nonlinear Dynamic Analysis of Structures in Three Dimensions, Version 960, Revision 1106, dated 01/28/2002.
- 5.3 LSTC, "LS-Post", version 2.0, revision 1622, dated July 17, 2002.
- 5.4 Standard Specification for Stainless Steel Bars and Shapes for Use in Boilers and Other Pressure Vessels, ASTM A479/A 479M -03.
- 5.5 The software "AutoSketch", by Autodesk, Inc, Release 2.1, October 5, 1995.
- 5.6 Harris, C. M, and Crede, C. E., "Shock and Vibration Handbook", Second Edition, McGraw Hill.

6.0 Analytical Model

The differences between the initial, detailed borobond model (described in Section 2.1) and the redesigned ES-3100 package are described in detail in Section 6.1. The material properties for the HABC are described in Section 6.2. Other than the geometric differences described in Section 6.1 and the material models described in Section 6.2, the detailed analytical models are the same as those presented in Part A, Section 2.1.

6.1 Model Description

The redesign configuration details to incorporate the HABC will be described as changes to the initial model. Figures 6.1 and 6.2 show the design configuration changes that were made in the analytical models. In the two figures, the black color indicates the initial design and the red (magenta) color indicates the redesign configuration.

The changes to the configuration of the analytical model were:

1. The internal radius of the liner between the neutron absorbing material and the kaolite was increased from 4.08 in to 4.30 in (Figure 6.1 and 6.2).
2. The internal radius of the liner above the neutron absorbing material and near the CV flange was decreased from 4.40 in to 4.30 in (Figure 6.1).
3. The radius of the CV bottom pad at its inner most part radius was increased from 0.05 in to 0.11 in. This effectively slightly thickens the pad at the footprint of the CV bottom head and therefore the CV was raised by about 0.068 in (Figure 6.1 and 6.2).

As a precipitate of the above configuration changes, some changes were made to the contact surfaces between the neutron absorber material, the kaolite and the stainless steel (SS) liners. The contact type remained the same as in the Part A computer runs (SURFACE_TO_SURFACE).

Figures 6.1.3 and 6.1.4 show the element mesh configurations near the CV flange and the CV bottom. These figures can be compared to Figures 2.1.3 and 2.1.4 to show the differences between the two design configurations.

The runs chosen to be made with the HABC modifications and compared to the original borobond model are shown in Figure 6.1.5. To differentiate the runs, yet show similarity,

the "HABC" is added to the borobond run identification to identify the redesign runs. For example, the Part A, borobond "run2e" impact configuration is known as "HABC-run2e" for the Part B, HABC runs.

Table 6.1.1 describes the impact configurations for the HABC computer runs. Note that the bounding stiffness runs (1hh and 1hl) do not include the punch impact following the crush impact. The Part A, 1hh and 1hl impacts and the punch study demonstrate the integrity of the drum/kaolite. The drum/kaolite remained the same for the Part B HABC runs, therefore the punch impacts were not included in the HABC runs. Table 6.1.1 also gives the kaolite and HABC models used in each run.

Table 6.1.2 shows the component mass/weight for the HABC models. The total weight for the fully loaded models is about 432 pounds with the 22.4 lb/ft³ kaolite. The mass inertia about the global Y axis is 90.98 in*lb*sec² and the CG is located at Z=22.41 inches above the bottom surface of the container.

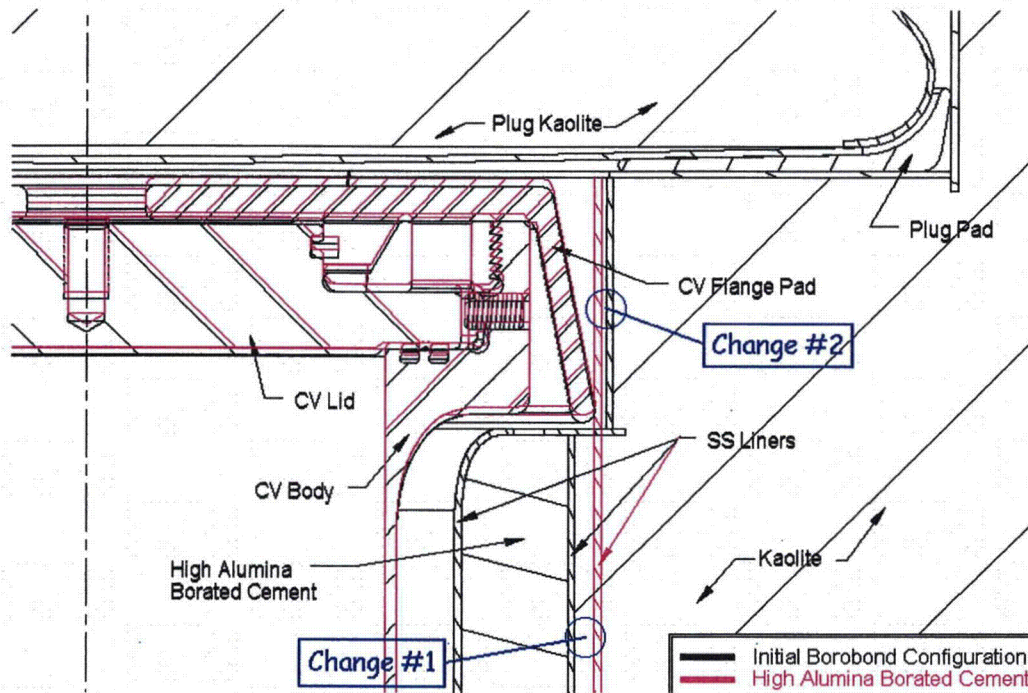


Figure 6.1.1 - Configuration Changes for the HABC, Compared to the Borobond Model Near the CV Flange

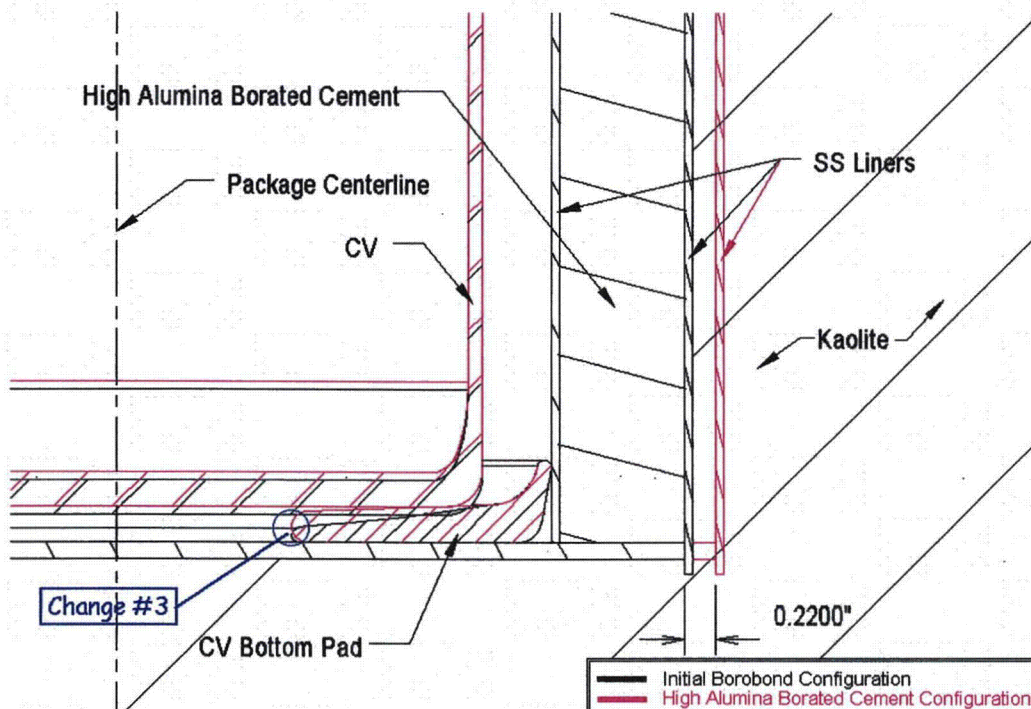


Figure 6.1.2 - Configuration Changes for the HABC, Compared to the Borobond Model Near the Bottom of the CV Body

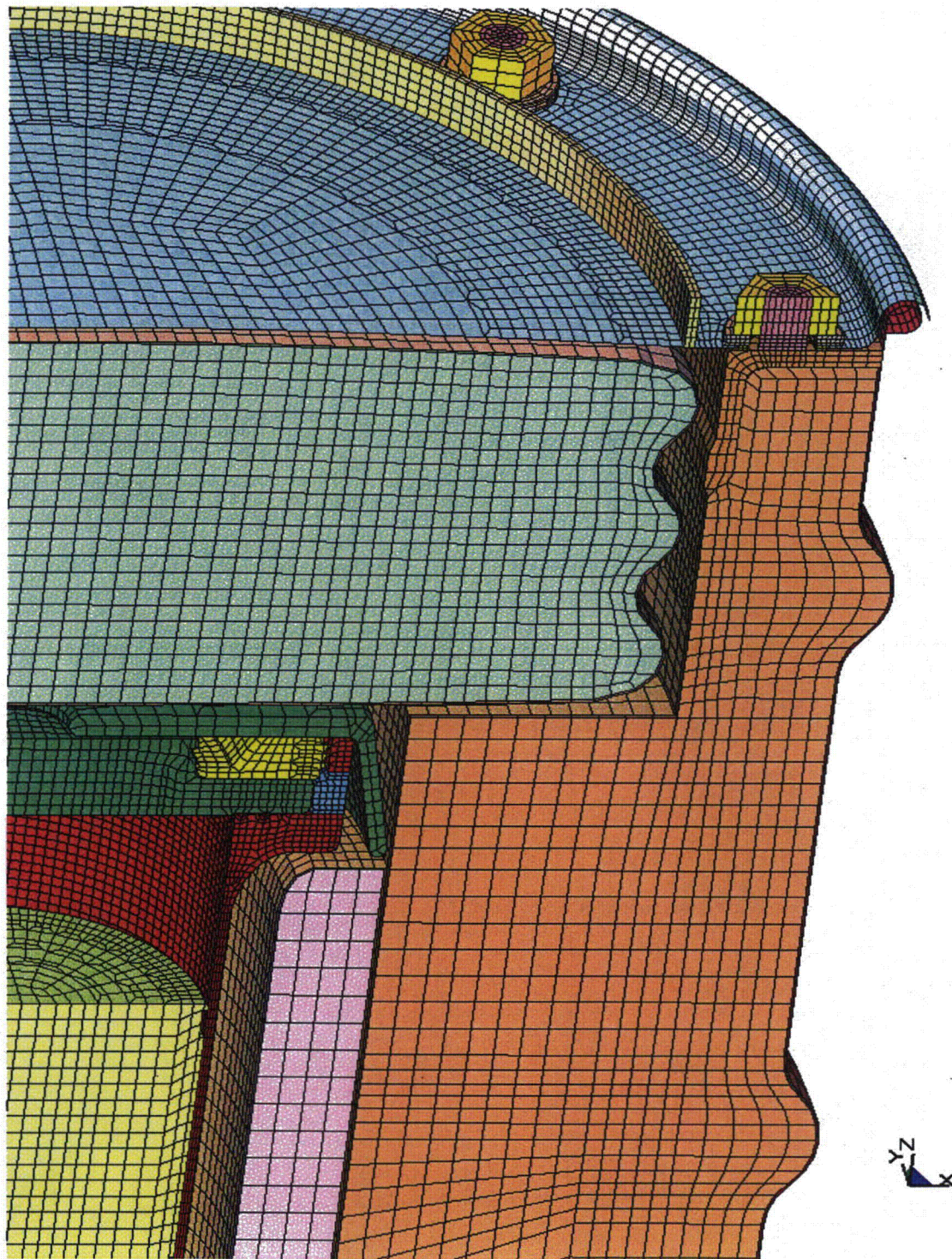


Figure 6.1.3 - Configuration of the HABC Analytical Model Near the Package Top

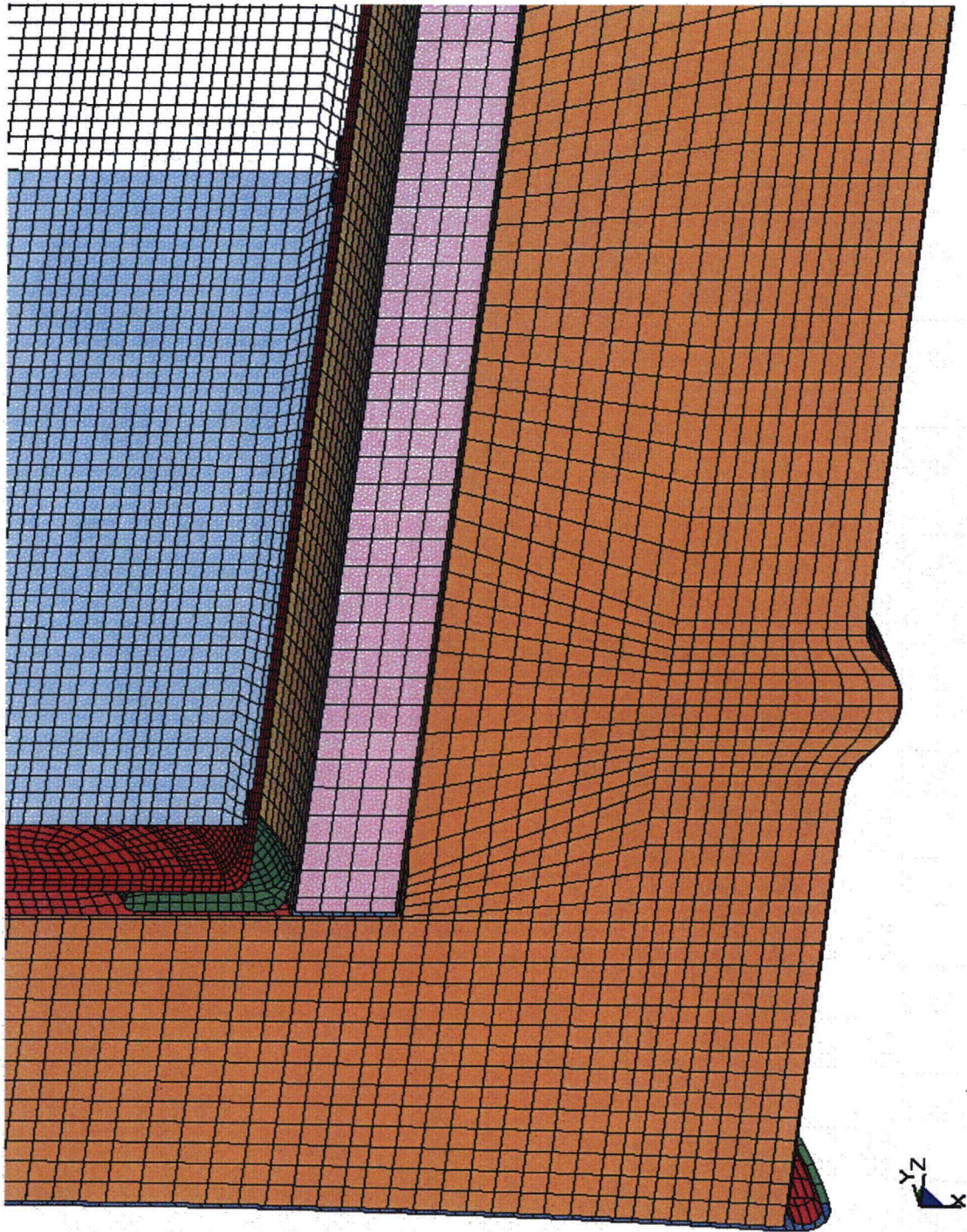


Figure 6.1.4 - Configuration of the HABC Analytical Model Near the Package Bottom

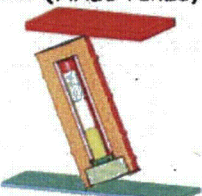
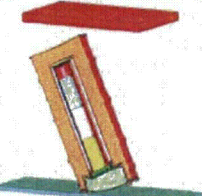
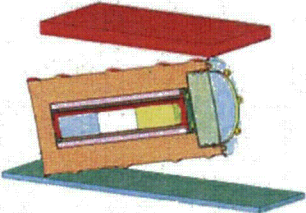
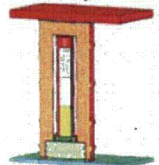
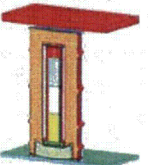
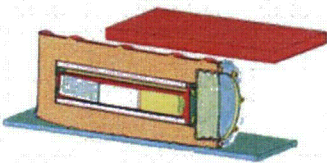
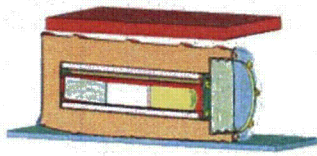
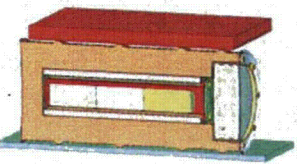
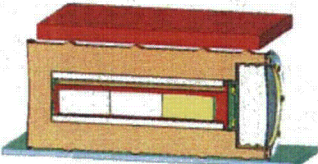
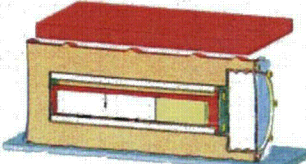
ES-3100 HABC Dynamic Analysis					
30-Foot Impact		Crush Impact		30-Foot Impact	
Lid Corner (HABC-run2e) 		Bottom Corner (HABC-run2e) 		12 Degree Slapdown (HABC-run4g, ga) 	
Top End Down (HABC-run3b) 		Bottom End Crush (HABC-run3b) 		Offset (HABC-run4g) 	
				Centered (HABC-run4ga) 	
4-Foot Impact		30-Foot Impact		Crush Impact	
Side (HABC-run1hl, 1hh) 		Side (HABC-run1hl, 1hh) 		Side (HABC-run1hl, 1hh) 	

Figure 6.1.5 - LS-Dyna Impact Configurations for the HABC Model

Table 6.1.1 - Description of the ES-3100 HABC Impacts			
Run ID	Impact Description	Kaolite Model	HABC Model
HABC-run1hl	4-foot side impact + 30-foot side impact + 30-foot crush impact	Lower bound stiffness, Section 3.2.5.2	100°F, Section 6.2.3
HABC-run1hh	4-foot side impact + 30-foot side impact + 30-foot crush impact	Upper bound stiffness, Section 3.2.5.3	-40°F, Section 6.2.1
HABC-run2e	30-foot CG over lid corner impact + 30-foot crush on bottom corner	Average stiffness, Section 3.2.5.1	70°F, Section 6.2.2
HABC-run3b	30-foot top end impact + 30-foot bottom end crush	Average stiffness, Section 3.2.5.1	70°F, Section 6.2.2
HABC-run4g	30-foot, 12° slapdown with lid studs on plane of symmetry + 30-foot crush with plate centered on CV flange	Average stiffness, Section 3.2.5.1	70°F, Section 6.2.2
HABC-run4ga	30-foot, 12° slapdown with lid studs on plane of symmetry + 30-foot crush with plate centered on drum	Average stiffness, Section 3.2.5.1	70°F, Section 6.2.2

Table 6.1.2 - Analysis Weights for the ES-3100 HABC Models

Material Number	Component Description	HABC-run2e			HABC-run1hh			HABC-run1hl			HABC-run3b			HABC-run4g		
		mass *	weight **	change***	mass	weight	change***	mass	weight	change***	mass	weight	change***	mass	weight	change***
m 1	CV body	2.73E-02	21.10	0.00	2.73E-02	21.10	0.00	2.73E-02	21.10	0.00	2.73E-02	21.10	0.00	2.73E-02	21.10	0.00
m 2	CV body at flange	1.73E-03	1.34	0.00	1.73E-03	1.34	0.00	1.73E-03	1.34	0.00	1.73E-03	1.34	0.00	1.73E-03	1.34	0.00
m 3	CV lid	9.57E-03	7.39	0.00	9.57E-03	7.39	0.00	9.57E-03	7.39	0.00	9.57E-03	7.39	0.00	9.57E-03	7.39	0.00
m 4	CV screw ring	4.27E-03	3.30	0.00	4.27E-03	3.30	0.00	4.27E-03	3.30	0.00	4.27E-03	3.30	0.00	4.27E-03	3.30	0.00
m 5	angle	1.69E-02	13.02	0.00	1.69E-02	13.02	0.00	1.69E-02	13.02	0.00	1.69E-02	13.02	0.00	1.69E-02	13.02	0.00
m 6	drum	6.02E-02	46.50	0.00	6.02E-02	46.50	0.00	6.02E-02	46.50	0.00	6.02E-02	46.50	0.00	6.02E-02	46.50	0.00
m 7	drum bottom head	1.22E-02	9.42	0.00	1.22E-02	9.42	0.00	1.22E-02	9.42	0.00	1.22E-02	9.42	0.00	1.22E-02	9.42	0.00
m 8	weld drum to drum bottom head	1.18E-04	0.09	0.00	1.18E-04	0.09	0.00	1.18E-04	0.09	0.00	1.18E-04	0.09	0.00	1.18E-04	0.09	0.00
m 9	liner overlap to angle (0.03)	1.36E-04	0.11	0.00	1.36E-04	0.11	0.00	1.36E-04	0.11	0.00	1.36E-04	0.11	0.00	1.36E-04	0.11	0.00
m 10	liner (0.06)	4.05E-02	31.23	0.71	4.05E-02	31.23	0.71	4.05E-02	31.23	0.71	4.05E-02	31.23	0.71	4.05E-02	31.23	0.71
m 11	liner bottom (0.120) (see m 27 for solids)	1.40E-03	1.08	0.00	1.40E-03	1.08	0.00	1.40E-03	1.08	0.00	1.40E-03	1.08	0.00	1.40E-03	1.08	0.00
m 12	lid shells (0.06)	7.25E-03	5.59	0.00	7.25E-03	5.59	0.00	7.25E-03	5.59	0.00	7.25E-03	5.59	0.00	7.25E-03	5.59	0.00
m 13	thin lid shell at bolts	1.37E-05	0.01	0.00	1.37E-05	0.01	0.00	1.37E-05	0.01	0.00	1.37E-05	0.01	0.00	1.37E-05	0.01	0.00
m 14	lid solids at the lid bolts	5.03E-05	0.04	0.00	5.03E-05	0.04	0.00	5.03E-05	0.04	0.00	5.03E-05	0.04	0.00	5.03E-05	0.04	0.00
m 15	lid stiffener	1.39E-03	1.07	0.00	1.39E-03	1.07	0.00	1.39E-03	1.07	0.00	1.39E-03	1.07	0.00	1.39E-03	1.07	0.00
m 16	drum bolts	5.06E-04	0.39	0.00	5.06E-04	0.39	0.00	5.06E-04	0.39	0.00	5.06E-04	0.39	0.00	5.06E-04	0.39	0.00
m 17	drum bolt nuts	1.20E-03	0.93	0.00	1.20E-03	0.93	0.00	1.20E-03	0.93	0.00	1.20E-03	0.93	0.00	1.20E-03	0.93	0.00
m 18	drum bolt washers	4.71E-04	0.36	0.00	4.71E-04	0.36	0.00	4.71E-04	0.36	0.00	4.71E-04	0.36	0.00	4.71E-04	0.36	0.00
m 19	plug liner	1.29E-02	10.00	0.00	1.29E-02	10.00	0.00	1.29E-02	10.00	0.00	1.29E-02	10.00	0.00	1.29E-02	10.00	0.00
m 20	plug kaolite	1.26E-02	9.70	0.00	1.52E-02	11.70	0.00	1.52E-02	11.70	0.00	1.26E-02	9.70	0.00	1.26E-02	9.70	0.00
m 21	drum kaolite	1.40E-01	107.88	-2.20	1.69E-01	130.43	-2.60	1.69E-01	130.43	-2.60	1.40E-01	107.88	-2.20	1.40E-01	107.88	-2.20
m 22	drum HABC	6.36E-02	49.08	5.38	6.36E-02	49.08	5.38	6.36E-02	49.08	5.38	6.36E-02	49.08	5.38	6.36E-02	49.08	5.38
m 24	lower internal cv mass	4.75E-02	36.69	0.00	4.75E-02	36.69	0.00	4.75E-02	36.69	0.00	4.75E-02	36.69	0.00	4.75E-02	36.69	0.00
m 25	middle internal cv mass	4.75E-02	36.69	0.00	4.75E-02	36.69	0.00	4.75E-02	36.69	0.00	4.75E-02	36.69	0.00	4.75E-02	36.69	0.00
m 26	upper internal cv mass	4.75E-02	36.69	0.00	4.75E-02	36.69	0.00	4.75E-02	36.69	0.00	4.75E-02	36.69	0.00	4.75E-02	36.69	0.00
m 27	liner bottom solids	1.25E-03	0.96	0.20	1.25E-03	0.96	0.20	1.25E-03	0.96	0.20	1.25E-03	0.96	0.20	1.25E-03	0.96	0.20
m 29	visual rigid plane	8.00E-04	0.62	-0.08	7.80E-04	0.60	0.00	7.80E-04	0.60	0.00	8.00E-04	0.62	0.00	9.00E-04	0.69	0.00
m 30	crush plate	1.42E+00	1099.99	0.00	1.42E+00	1099.99	0.00	1.42E+00	1099.99	0.00	1.42E+00	1099.99	0.00	1.42E+00	1099.99	0.00
m 31	punch	8.24E-02	63.62	0.00	8.24E-02	63.62	0.00	8.24E-02	63.62	0.00	8.24E-02	63.62	0.00	8.24E-02	63.62	0.00
m32	silicon rubber	1.74E-03	1.34	0.07	1.74E-03	1.34	0.07	1.74E-03	1.34	0.07	1.74E-03	1.34	0.07	1.74E-03	1.34	0.07
	dyna total model weight	2.07E+00	1596.23	4.09	2.10E+00	1620.77	3.77	2.10E+00	1620.77	3.77	2.07E+00	1596.23	4.16	2.07E+00	1596.31	4.16
	CV lid and nut ring		10.68			10.68			10.68			10.68			10.68	
	CV body wt		22.44			22.44			22.44			22.44			22.44	
	CV total wt		33.12			33.12			33.12			33.12			33.12	
	plug liner and kaolite		19.70			21.69			21.69			19.70			19.70	
	liner + angle		46.41			46.41			46.41			46.41			46.41	
	drum body + kaolite + borobond4		261.10			263.66			263.66			261.10			261.10	
	drum + lid + plug + kaolite + borobond4		288.81			313.36			313.36			288.81			288.81	
	internal cv masses		110.08			110.08			110.08			110.08			110.08	
	Total Package Weight		432.01			456.56			456.56			432.01			432.01	
	Crush Plate Weight		1099.99			1099.99			1099.99			1099.99			1099.99	
	Punch Weight		63.62			63.62			63.62			63.62			63.62	
	Visual Rigid Plane		0.62			0.60			0.60			0.62			0.69	
	Total Model Weight		1596.23			1620.77			1620.77			1596.23			1596.31	

* - Mass is for the 1/2 model and is the units of (pound* second^2)/inch
 ** - Weight is for the total package (2* model weight) and is in units of pounds
 *** - Change is the difference between the HABC run and the Table 2.1.2 results

6.2 Material Models

The material models used in the Part B HABC runs are those described in the Part A, Section 2.3 except for the Section 2.3.6 which covered the Borobond material. As in the initial borobond models the stud material was defined with a material failure at the 0.57 in/in strain level.

The borobond material was replaced with the catalog 277-4 high alumina borated cement material which is described in this section and sub-sections. The LS-Dyna material model used for the HABC material is the *MAT_SOIL_AND_FOAM model. The material data was obtained from testing performed at Y12 in the Fall of 2004. Figure 6.2.1 shows the stress vs strain curves obtained in the test.

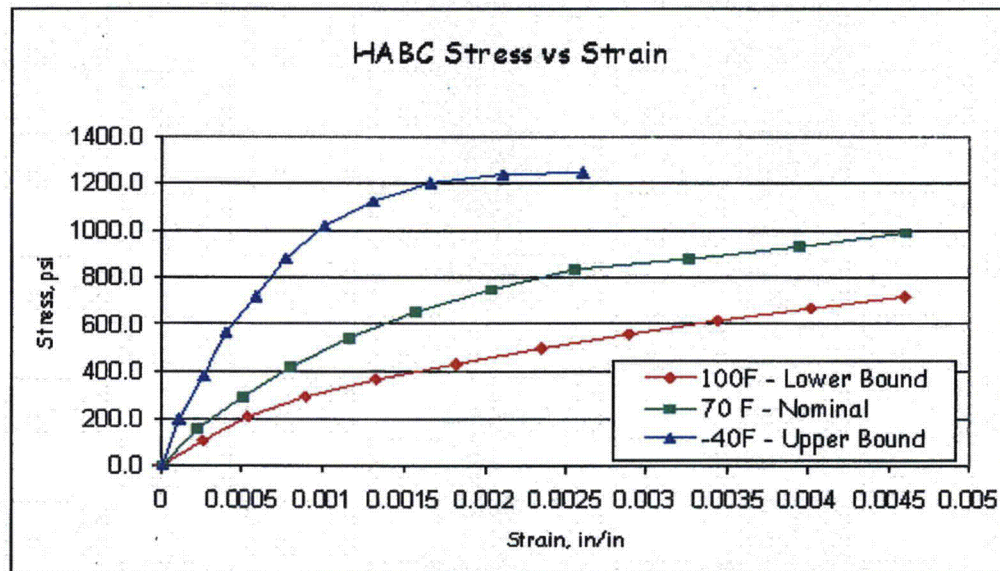


Figure 6.2.1 - HABC Stress vs Strain Curves

6.2.1 HABC at -40° F

Poisson's ratio is given as 0.33 by the testing results. The modulus of elasticity was taken to be the slope of the load deflection curve for the first data point.

$$E = \frac{\sigma}{\epsilon} = \frac{201.3 \text{ psi} - 0 \text{ psi}}{(101.1 \times 10^{-6}) - 0} = 1.991 \text{e}6 \text{ psi}$$

The shear modulus is then calculated as:

$$\text{Shear Modulus} = \frac{E}{2(1+\nu)} = \frac{1.991 \text{e}6 \text{ psi}}{2(1+0.33)} = 7.485 \text{e}5 \text{ psi}$$

The bulk modulus is calculated as:

$$\text{BulkModulus} = \frac{E}{3(1-2\nu)} = \frac{1.991e6 \text{ psi}}{3(1+2(0.33))} = 1.952e6 \text{ psi}$$

Volumetric response data for the HABC material is lacking. A volumetric response will be derived from the one dimensional compressive test data. The HABC material is assumed to behave as a homogeneous, isotropic material.

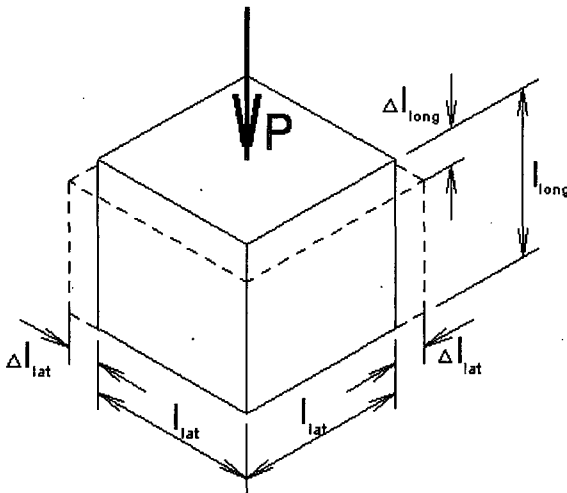


Figure 6.2.1.1 - Assumed Response of a Unit Cube

Using Figure 6.2.1.1 and noting the following definitions,

$$\epsilon_{long} = \frac{\Delta l_{long}}{l_{long}} ; \epsilon_{lat} = \frac{\Delta l_{lat}}{l_{lat}} ; \nu = \frac{\epsilon_{lat}}{\epsilon_{long}}$$

$$\epsilon_{lat} = \nu \epsilon_{long}$$

$$l_{lat} = l_{long} = l$$

The initial volume is, l^3 , and the final volume is:

$$\text{final volume} = (l - \Delta l_{long})(l + \Delta l_{lat})(l + \Delta l_{lat})$$

Substituting the above definitions into this equation and simplifying results in the following expression for the final volume.

$$\text{final volume} = l^3(1 - \epsilon_{long})(1 + \nu\epsilon_{long})^2$$

The relative volume then is,

$$V = \frac{\text{current volume}}{\text{initial volume}} = (1 - \epsilon_{long})(1 + \nu\epsilon_{long})^2$$

The volumetric strain then is:

$$\text{volumetric strain} = \ln V$$

Using this and $P = \sigma/3$, a pressure vs volumetric strain curve is derived. The pressure cut off for tension is derived from the tensile failure of 234.7 psi. The pressure cut off for the material model is: $P = \frac{\sigma}{3} = \frac{234.7 \text{ psi}}{3} = 78.2 \text{ psi}$.

The constants a_0 , a_1 , and a_2 are yield function constants defined in the material model. To eliminate the pressure dependence of the yield strength, $a_1 = a_2 = 0$ and $a_0 = \sigma_y^2/3 = (1165.8 \text{ psi})^2/3 = 4.530e5 \text{ psi}^2$. The following material model was used for the upper stiffness bound of the HABC material (-40°).

LS-Dyna Material Model	*MAT_SOIL_AND_FOAM
Density	1.5742e-4 lb-sec ² /in ⁴ (105 lb/ft ³)
Shear Modulus	7.485e5 psi
Bulk Modulus	1.952e6 psi
A ₀	4.530e5 (psi) ²
A ₁	0
A ₂	0
Tensile Cutoff	78.2 psi

Volumetric Strain Data vs Pressure:

<u>Volumetric Strain, in³/in³</u>	<u>Pressure, psi</u>
0	0
-3.4380E-05	67.100
-1.3300E-04	187.300
-2.5971E-04	294.367
-4.4481E-04	374.067
-8.8812E-04	416.567
-3.4612E-03 [†]	433.333 [†]
-1.6787E-01 [†]	566.667 [†]
-5.5498E-01 [†]	1000.000 [†]
-1.1409E+00 [†]	100000.000 [†]

† - assumed values to achieve numerical lock-up.

6.2.2 HABC at 70° F

Poisson's ratio is given as 0.28 by the testing. The modulus of elasticity was taken to be the slope of the load deflection curve for the first data point.

$$E = \frac{\sigma}{\varepsilon} = \frac{150.3 \text{ psi} - 0 \text{ psi}}{(219.8e-6) - 0} = 6.838e5 \text{ psi}$$

The shear modulus is then calculated as:

$$\text{Shear Modulus} = \frac{E}{2(1+\nu)} = \frac{6.838e5 \text{ psi}}{2(1+0.28)} = 2.671e5 \text{ psi}$$

The bulk modulus is calculated as:

$$\text{Bulk Modulus} = \frac{E}{3(1-2\nu)} = \frac{6.838e5 \text{ psi}}{3(1+2(0.28))} = 5.180e5 \text{ psi}$$

The pressure cut off is calculated as $P=184 \text{ psi} / 3 = 61.3 \text{ psi}$ and the constants a_0 is calculated as $(983 \text{ psi})^2 / 3 = 3.221e5 \text{ psi}^2$. The following material model was used for the 70°F runs of the HABC material.

LS-Dyna Material Model	*MAT_SOIL_AND_FOAM
Density	1.5742e-4 lb-sec ² /in ⁴ (105 lb/ft ³)
Shear Modulus	2.671e5 psi
Bulk Modulus	5.180e5 psi
A ₀	3.221e5 (psi) ²
A ₁	0
A ₂	0
Tensile Cutoff	61.3 psi

Volumetric Strain Data vs Pressure:

<u>Volumetric Strain, in³/in³</u>	<u>Pressure, psi</u>
0.0000E+00	0.000
-9.6740E-05	50.100
-3.5131E-04	140.400
-6.9019E-04	217.100
-1.1268E-03	278.133
-2.0363E-03	329.067
-1.9536E-01 [†]	500.000 [†]
-6.0570E-01 [†]	1000.000 [†]
-8.4601E-01 [†]	10000.000 [†]
-1.2052E+00 [†]	100000.000 [†]

† - assumed values to achieve numerical lock-up.

6.2.3 HABC at 100° F

Poisson's ratio is given as 0.25. The modulus of elasticity was taken to be the slope of the load deflection curve for the first data point.

$$E = \frac{\sigma}{\epsilon} = \frac{103.7 \text{ psi} - 0 \text{ psi}}{(257.5e-6) - 0} = 4.027e5 \text{ psi}$$

The shear modulus is then calculated as:

$$\text{Shear Modulus} = \frac{E}{2(1+\nu)} = \frac{4.027e5 \text{ psi}}{2(1+0.25)} = 1.6108e5 \text{ psi}$$

The bulk modulus is calculated as:

$$\text{Bulk Modulus} = \frac{E}{3(1-2\nu)} = \frac{4.027e5 \text{ psi}}{3(1+2(0.25))} = 2.6847e5 \text{ psi}$$

The pressure cut off is calculated as $P = 209.7 \text{ psi} / 3 = 69.9 \text{ psi}$ and the constants a_0 is calculated as $(833.7 \text{ psi})^2 / 3 = 2.317e5 \text{ psi}^2$. The following material model was used for the lower bound, 100° F runs of the HABC material.

LS-Dyna Material Model	*MAT_SOIL_AND_FOAM
Density	1.5742e-4 lb-sec ² /in ⁴ (105 lb/ft ³)
Shear Modulus	1.6108e5 psi
Bulk Modulus	2.6847e5 psi
A ₀	2.317e5 (psi) ²
A ₁	0
A ₂	0
Tensile Cutoff	69.9 psi

Volumetric Strain Data vs Pressure:

<u>Volumetric Strain, in³/in³</u>	<u>Pressure, psi</u>
0.0000E+00	0.0
-1.2879E-04	34.567
-6.6103E-04	123.133
-1.1769E-03	165.533
-1.7225E-03	204.967
-2.3119E-03	240.0
-5.5975E-02 [†]	333.333 [†]
-4.5758E-01 [†]	500.0 [†]
-6.3677E-01 [†]	1000.0 [†]
-1.2448E+00 [†]	100000.0 [†]

† - assumed values to achieve numerical lock-up.

The volumetric strain vs pressure curves used by the analytical models are plotted in Figure 6.2.3.1 for the lower values.

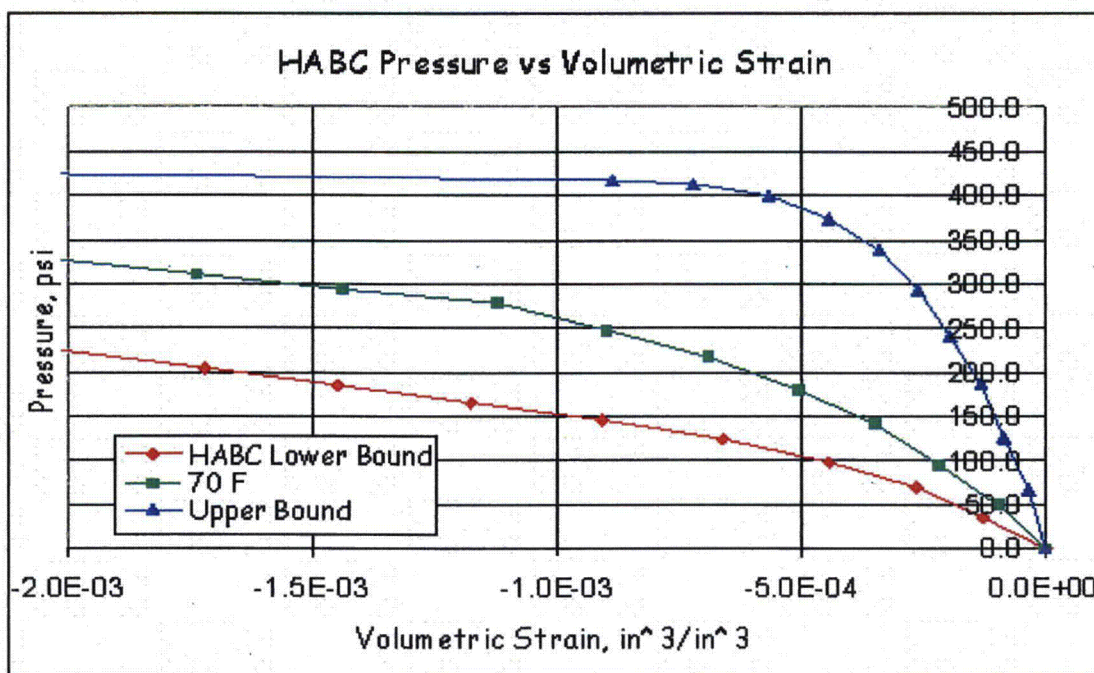


Figure 6.2.3.1 - Volumetric Strain vs Pressure Curves for the HABC Material

7.0 Analysis Results

The figures presented in Section 7 may show the punch, however, no punch impacts were made on the HABC model as discussed in Section 6.1.

7.1 HABC-run1hl - Lower Bounding Side

HABC-run1hl are the runs with the lower bounding material properties for the kaolite and the HABC materials. The 4-foot impact occurs from time = 0.0 to 0.01 seconds; the 30-foot impact occurs from 0.01 to 0.02 seconds; and the crush impact occurs from 0.02 to 0.04 seconds.

The initial configuration for HABC-run1hl is shown in Figure 7.1.1. The configuration after the 4-foot impact is shown in Figure 7.1.2. Enlargement of the lid and bottom regions after the 4-foot impact is shown in Figure 7.1.3.

The effective plastic strain in the CV body after the 4-foot impact is shown in Figure 7.1.4. The maximum is 0.0185 in/in and occurs near the bottom head of the CV body. The plastic strain in other components for the 4-foot impact are given in Table 7.1.1.

Component	Effective Plastic Strain, in/in
CV Lid	0.0001
CV Nut Ring	0.0000
Angle	0.0055
Drum	0.1599
Drum Bottom Head	0.1033
Liner	0.1045
Lid	0.1393
Lid Stiffener	0.0004
Lid Studs	0.0000
Lid Stud Nuts	0.0000
Lid Stud Washers	0.0194
Plug Liner	0.0022

Figure 7.1.5 shows the final configuration for the HABC-run1hl 30-foot impact. Figure 7.1.6 shows the lid and bottom regions after the 30-foot impact.

The maximum effective plastic strain due to the 30-foot impact in the CV body is 0.0195 in/in as shown in Figure 7.1.7. The maximum effective plastic strain in the drum lid is shown to be 0.5790 in/in in Figure 7.1.8. The maximum lid strain is a surface strain at the stud hole nearest the rigid surface. The membrane effective plastic strain component is 0.4416 in/in in the localized region near the stud hole. Effective plastic strain levels in other components for the 30-foot impact are given in Table 7.1.2.

Component	Effective Plastic Strain, in/in
CV Lid	0.0002
CV Nut Ring	0.0000
Angle	0.0780
Drum	0.2251
Drum Bottom Head	0.2126
Liner	0.1078
Lid Stiffener	0.0093
Lid Studs	0.1140
Lid Stud Nuts	0.0000
Lid Stud Washers	0.0194
Plug Liner	0.0958

The final configuration for the crush impact is shown in Figure 7.1.9. Figure 7.1.10 shows the configuration at the bottom and lid regions after the crush impact.

Figure 7.1.11 shows the effective plastic strains in the CV body. The maximum is shown to be 0.0206 in/in and occurs below the flange region due to the upper internal weight.

The maximum effective plastic strain in the drum for the crush impact is 0.5139 in/in (surface strain) as shown in Figure 7.1.12. The maximum in the drum occurs near the angle on the crush plate side of the drum. The maximum membrane effective plastic strain at this location is 0.3551 in/in.

Figure 7.1.13 shows that the maximum effective plastic strain in the lid is 1.2580 in/in (surface strain) and occurs just below the upper stud hole (hole nearest the crush plate, 180°). The maximum membrane effective plastic strain in this region of the lid is 0.7746 in/in. A time line investigation during the crush impact shows that the lid exceeds 0.57 in/in strain in bending at about 0.0248 seconds at the 180° stud hole. The crush impact started at about 0.0200 seconds, so the lid reaches failure level near the start of the crush impact. The membrane levels in the lid reach 0.57 in/in at about 0.0264 seconds. The elevated effective plastic strain levels in the lid are localized in the region just inboard of the upper stud.

Figure 7.1.14 shows that the effective plastic strain in the drum studs is 0.5121 in/in and occurs in the upper stud at the bearing of the lid onto the stud. The elevated strains in the stud are localized on the inner surface (bearing of the lid on the stud). Effective plastic strain levels throughout the thickness of the stud are generally 0.25 in/in or less. At time 0.0264 sec, the lid has reached 0.57 in/in strain in membrane, and the maximum strain in the drum studs is about 0.2870 in/in.

Considering the strain levels in the lid and the studs, some tearing at the 180° stud hole would be expected. But the tearing would be localized to the stud hole due to the extent of the strain patterns. Failure of the stud to restrain the lid due to this tearing is not expected. The lid stiffener would limit any tearing from the stud at 180° and the large washer would be expected to restrain the lid. The effective plastic strain in other components due to the crush impact are listed in Table 7.1.3.

Table 7.1.3 - HABC-run1hl, Crush Impact, Effective Plastic Strain Levels in Some Components	
Component	Effective Plastic Strain, in/in
CV Lid	0.0002
CV Nut Ring	0.0000
Angle	0.1142
Drum Bottom Head	0.3562
Liner	0.1593
Lid Stiffener	0.0515
Lid Stud Nuts	0.0005
Lid Stud Washers	0.0693
Plug Liner	0.1220

The lid separation time history is shown in Figure 7.1.15. The nodes used in Figure 7.1.15 are shown in Figure 3.1.30. From the time history plot it can be seen that a lid separation of 0.005 in or less would be expected.

Figure 7.1.16 shows kaolite nodes used to find the kaolite thickness time history. Figure 7.1.17 shows the remaining thickness time histories for the nodal pairs shown.

Figure 7.1.18 and 7.1.19 show the diameter and radial time histories for the drum. The nodes are defined in Figure 3.1.34.

Figure 7.1.20 shows the diameter time history for nodal pairs along the length of the liner. Figure 3.1.37 shows the nodes and Table 3.1.3 gives the location of the nodes.

3100 HABC-RUN1HL L BOUND DEC 2004 KQH
Time = 0

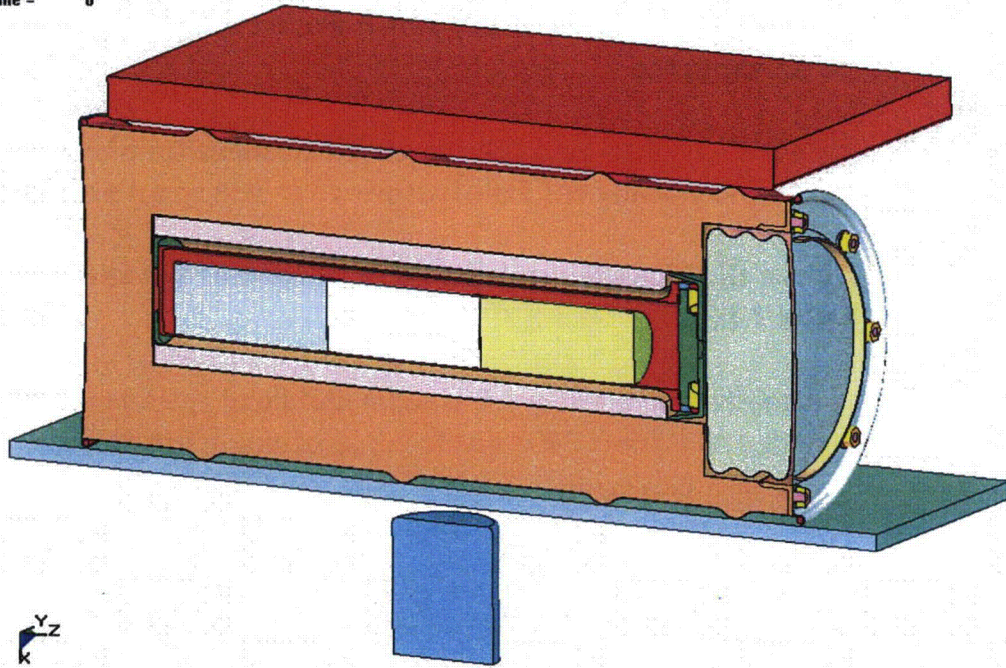


Figure 7.1.1 - HABC-run1hl, Initial Configuration

3100 HABC-RUN1HL L BOUND DEC 2004 KQH
Time = 0.01

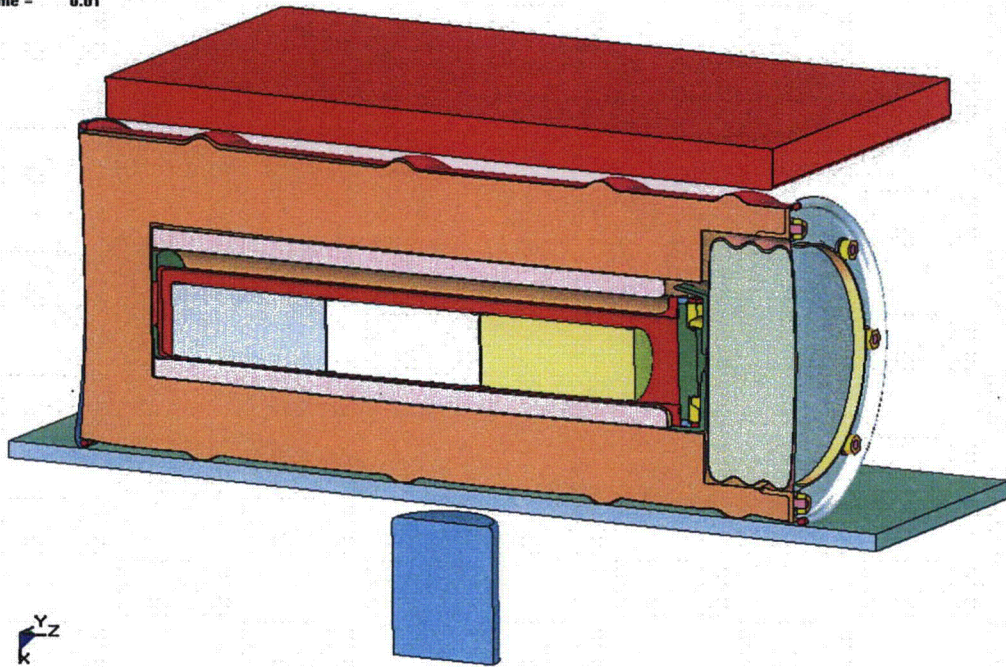


Figure 7.1.2 - HABC-run1hl, Configuration After the 4-Foot Impact

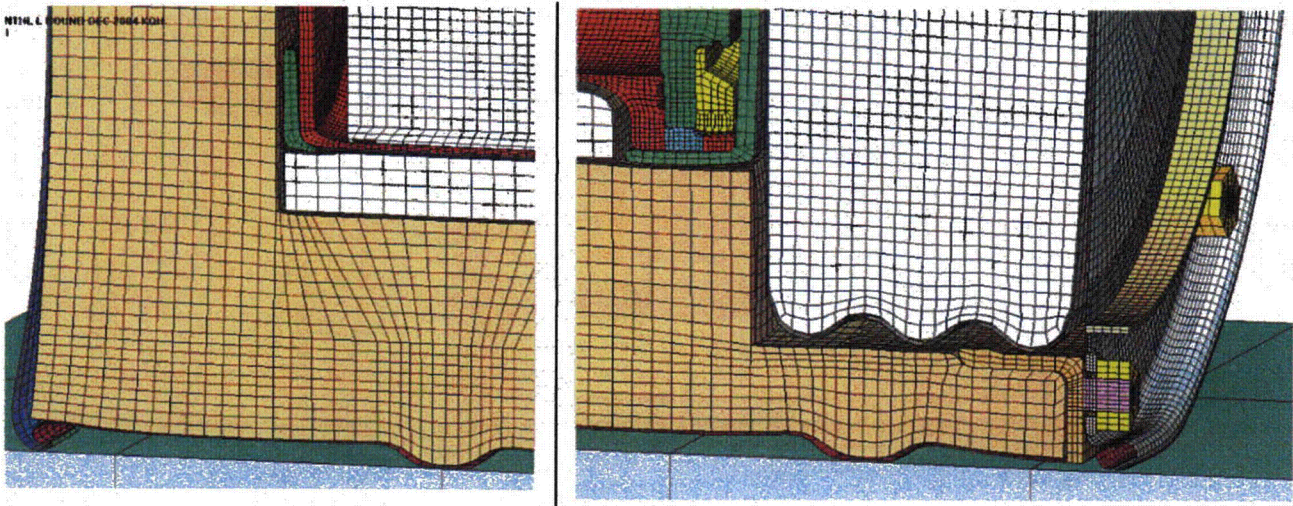


Figure 7.1.3 - HABC-run1hl, 4-Foot Impact, Configuration in the Lid and Bottom

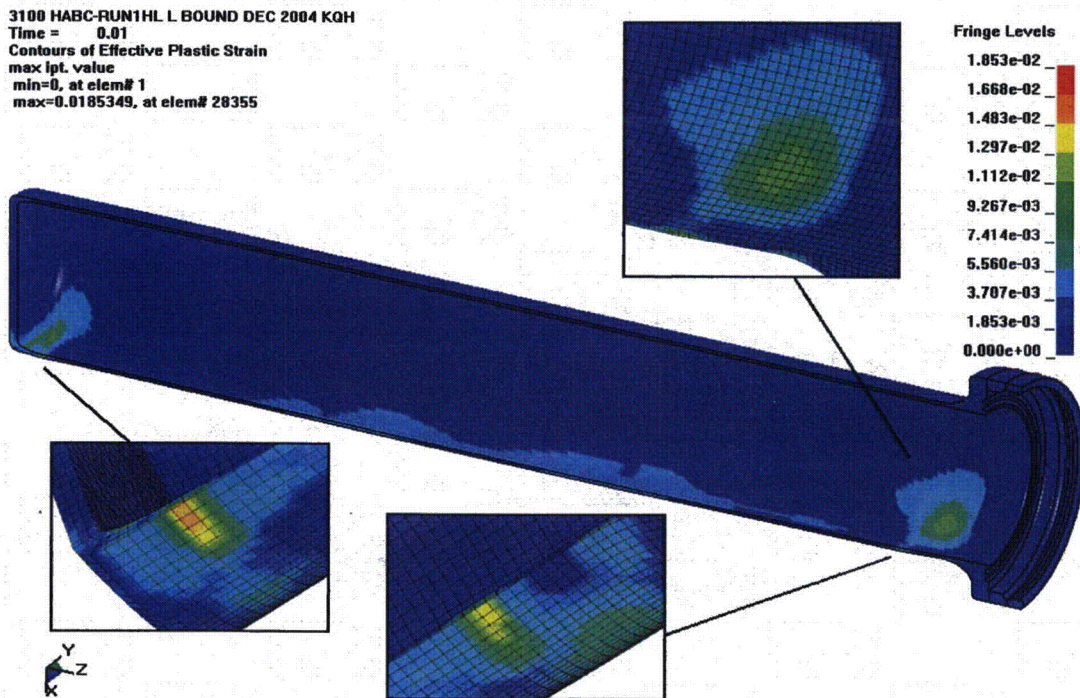


Figure 7.1.4 - HABC-run1hl, 4-Foot Impact, Effective Plastic Strain in the CV Body

3100 HABC-RUN1HL L BOUND DEC 2004 KQH
Time = 0.020001

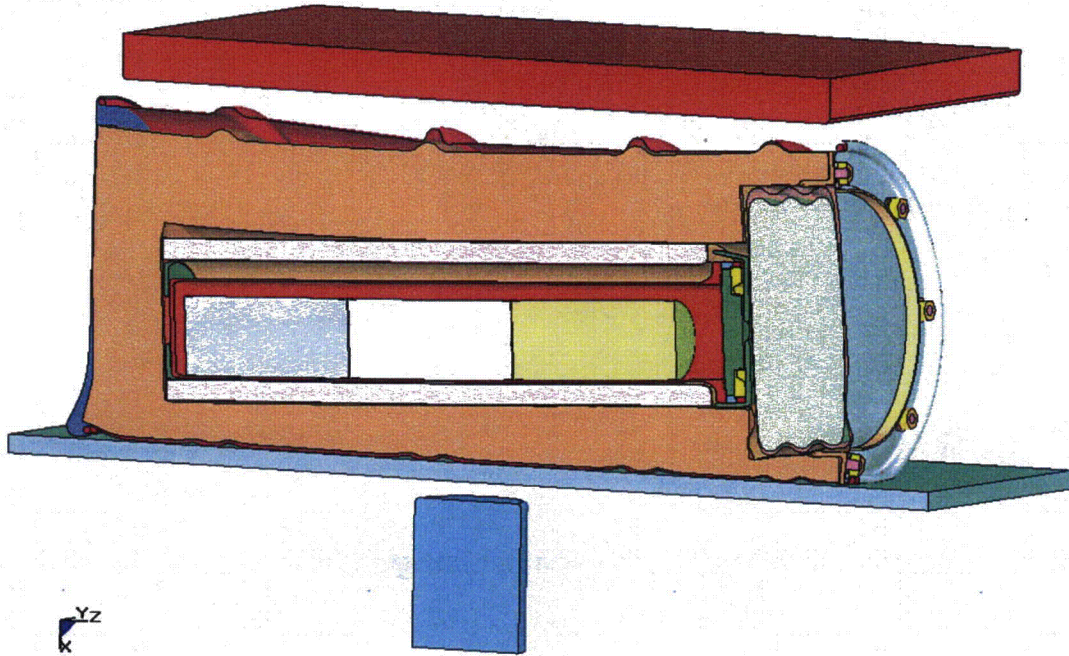


Figure 7.1.5 - HABC-run1hl, 30-Foot Impact, Final Configuration

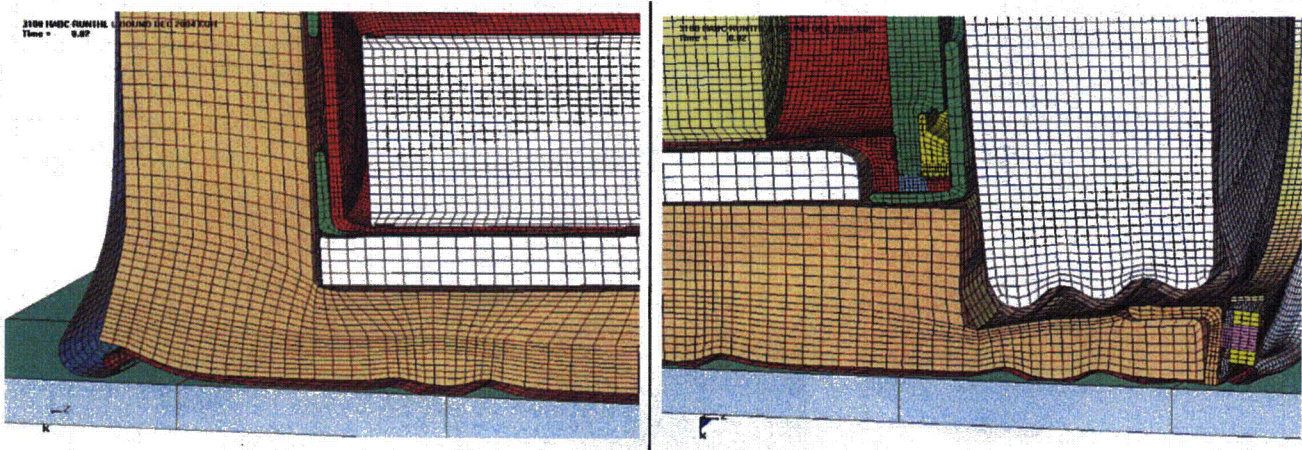


Figure 7.1.6 - HABC-run1hl, 30-Foot Impact, Configuration of the Lid and Bottom

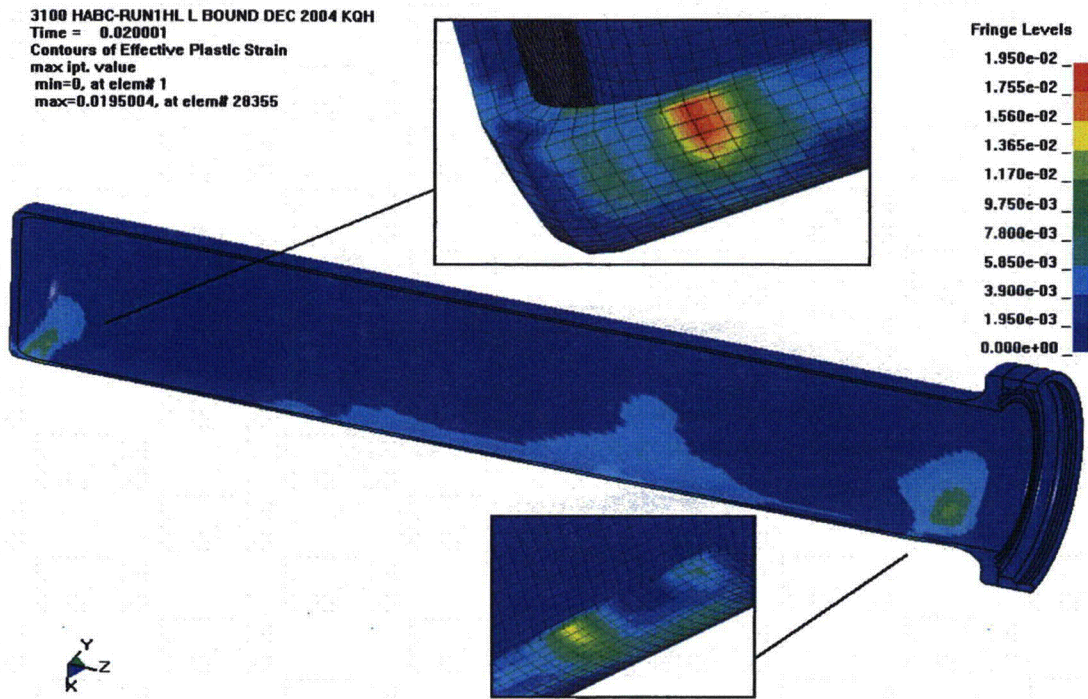


Figure 7.1.7 - HABC-run1hl, 30-Foot Impact, Effective Plastic Strain in the CV Body

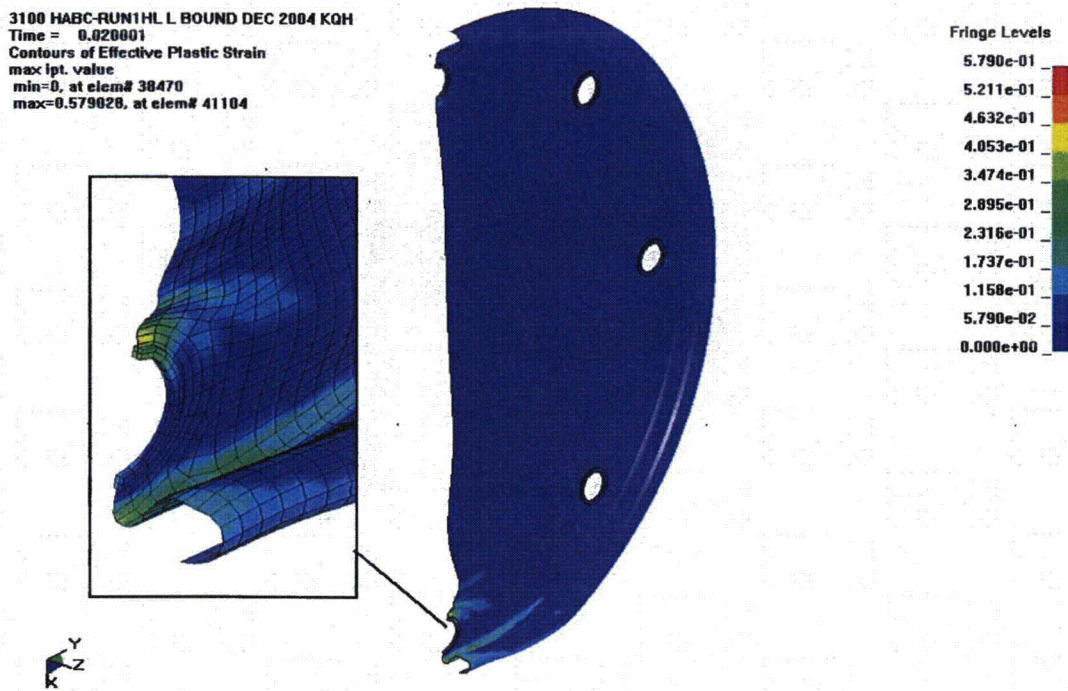


Figure 7.1.8 - HABC-run1hl, 30-Foot Impact, Effective Plastic Strain in the Lid

3100 HABC-RUN1HL L BOUND DEC 2004 KQH
Time = 0.04

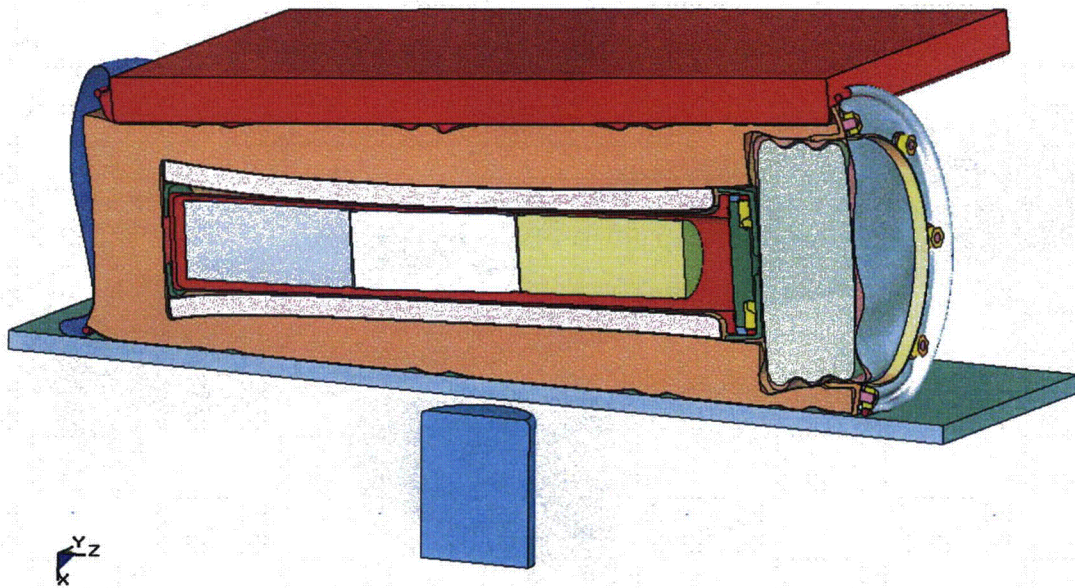


Figure 7.1.9 - HABC-run1hl, Crush Impact, Final Configuration

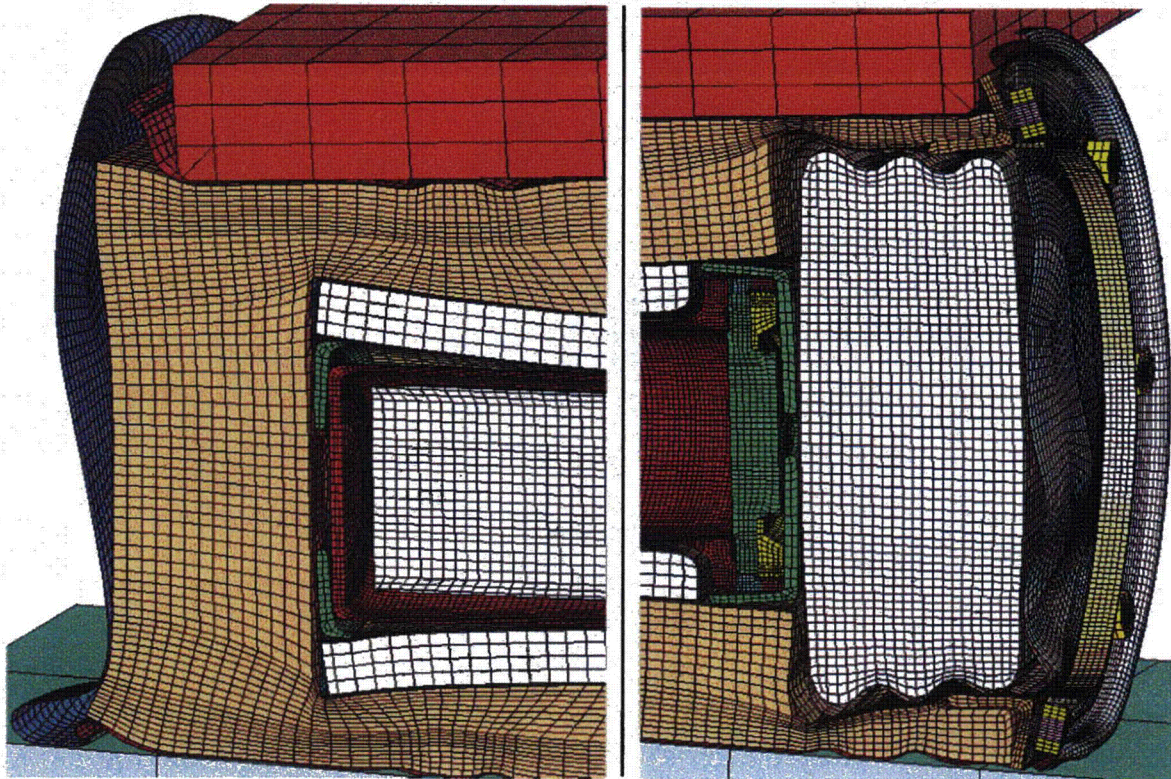


Figure 7.1.10 - HABC-run1hl, Crush Impact, Configuration of the Lid and Bottom

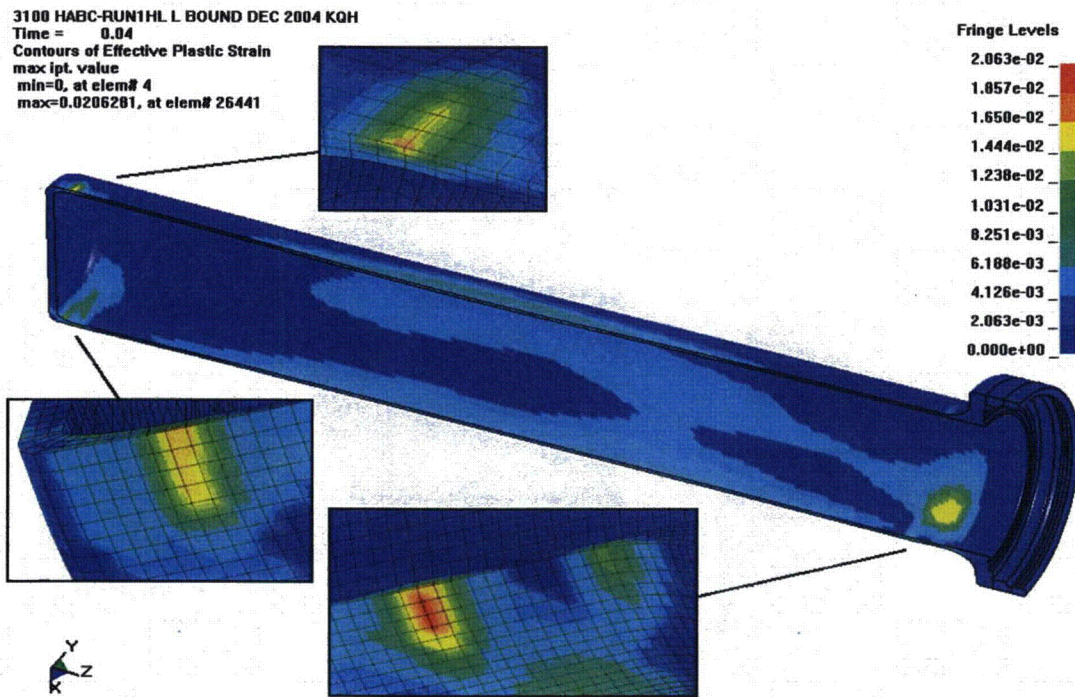


Figure 7.1.11 - HABC-run1hl, Crush Impact, Effective Plastic Strain in the CV Body

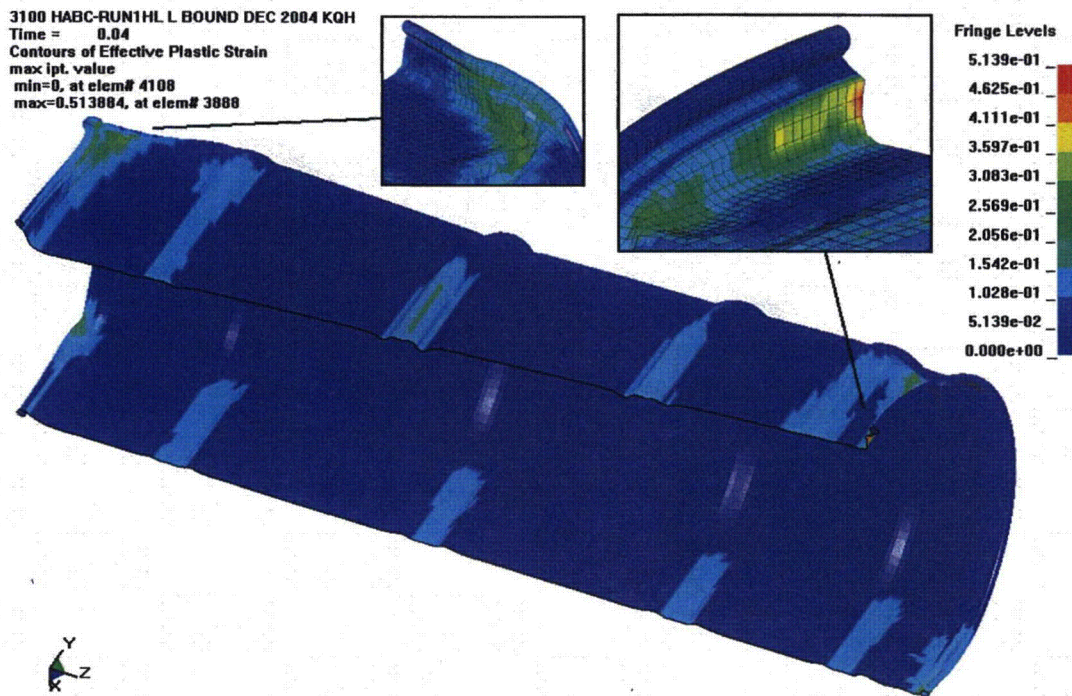


Figure 7.1.12 - HABC-run1hl, Crush Impact, Effective Plastic Strain in the Drum

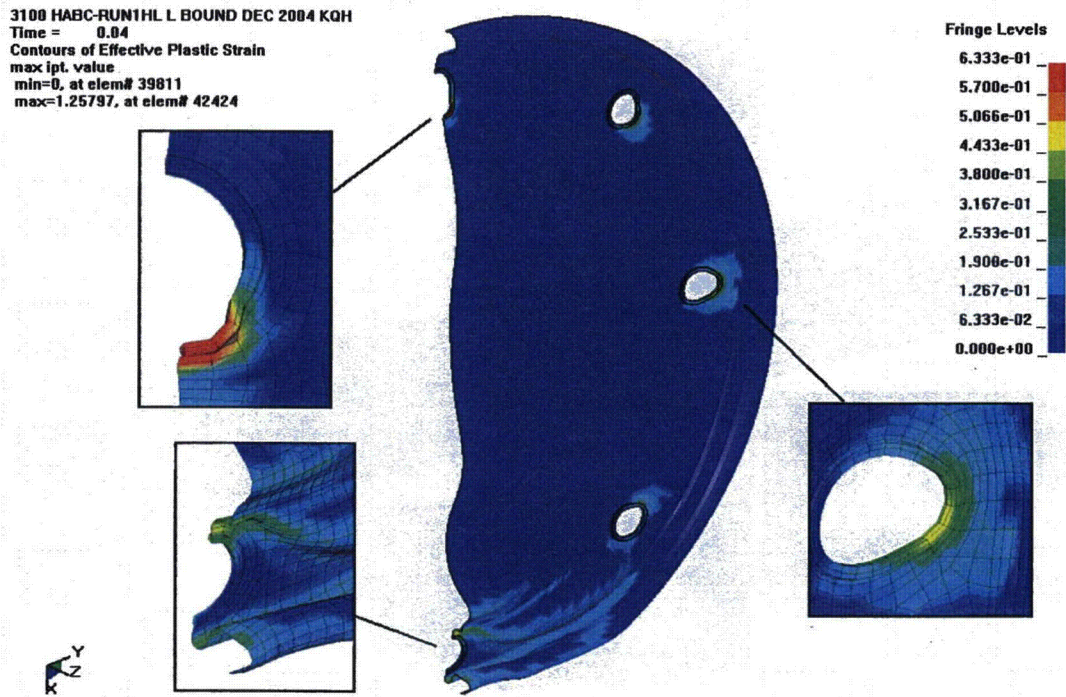


Figure 7.1.13 - HABC-run1hl, Crush Impact, Effective Plastic Strain in the Lid

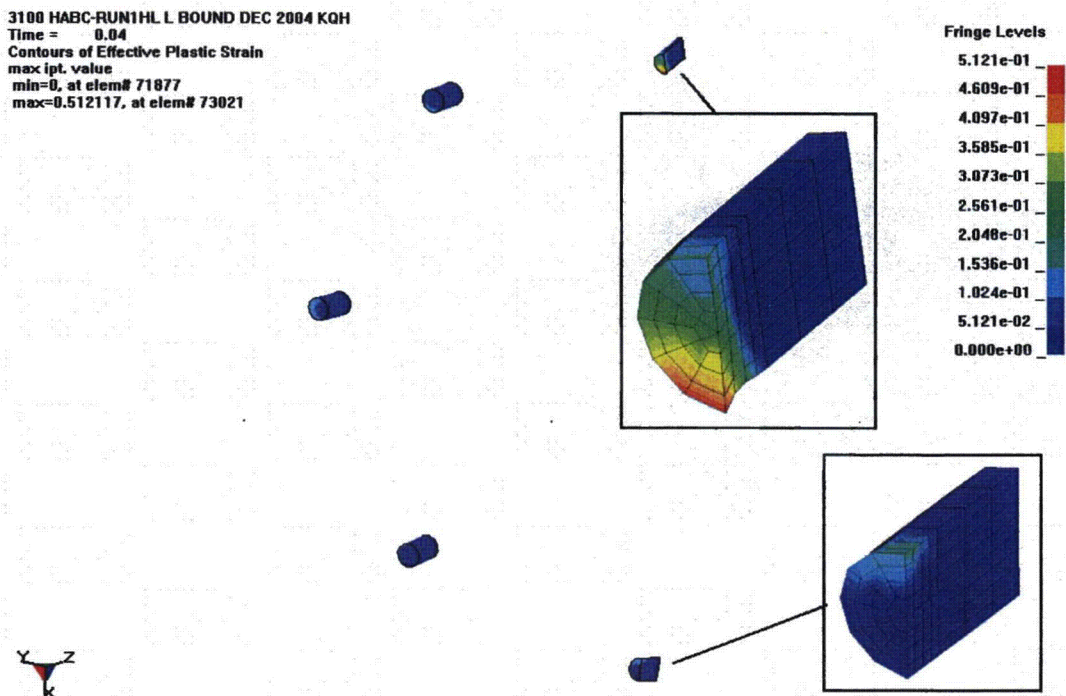


Figure 7.1.14 - HABC-run1hl, Crush Impact, Effective Plastic Strain in the Studs

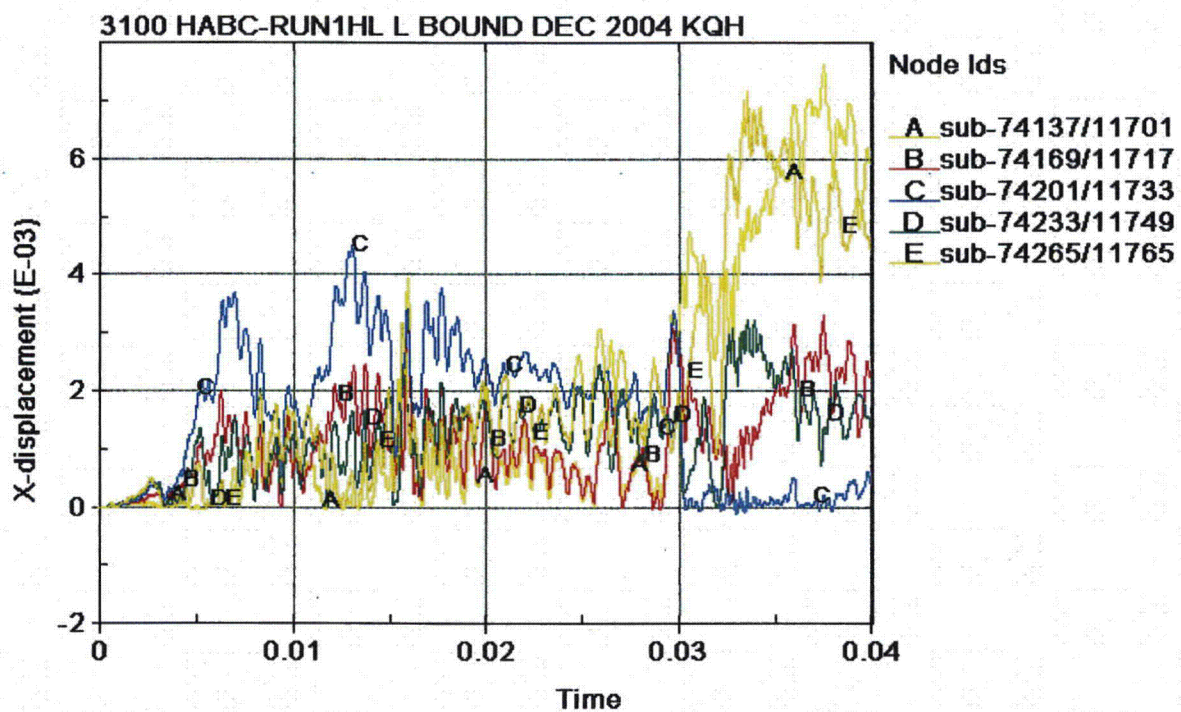


Figure 7.1.15 - HABC-run1hl, CV Lid Separation Time History

3100 HABC-RUN1HL L BOUND DEC 2004 KQH
Time = 0

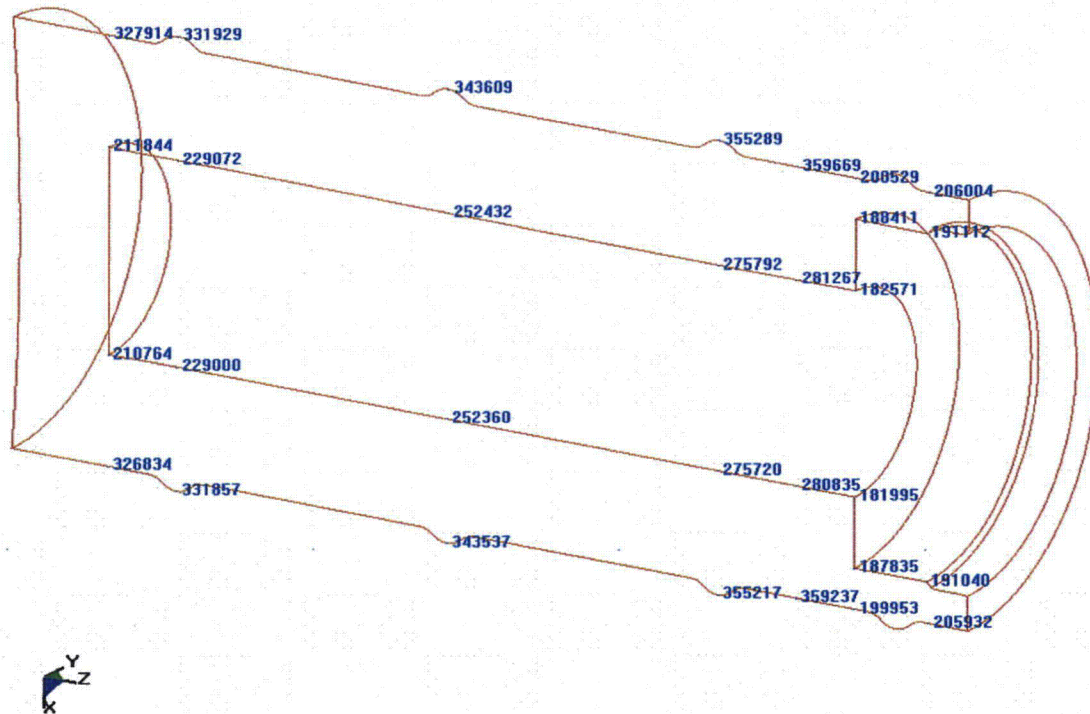


Figure 7.1.16 - HABC-run1hl, Kaolite Nodes

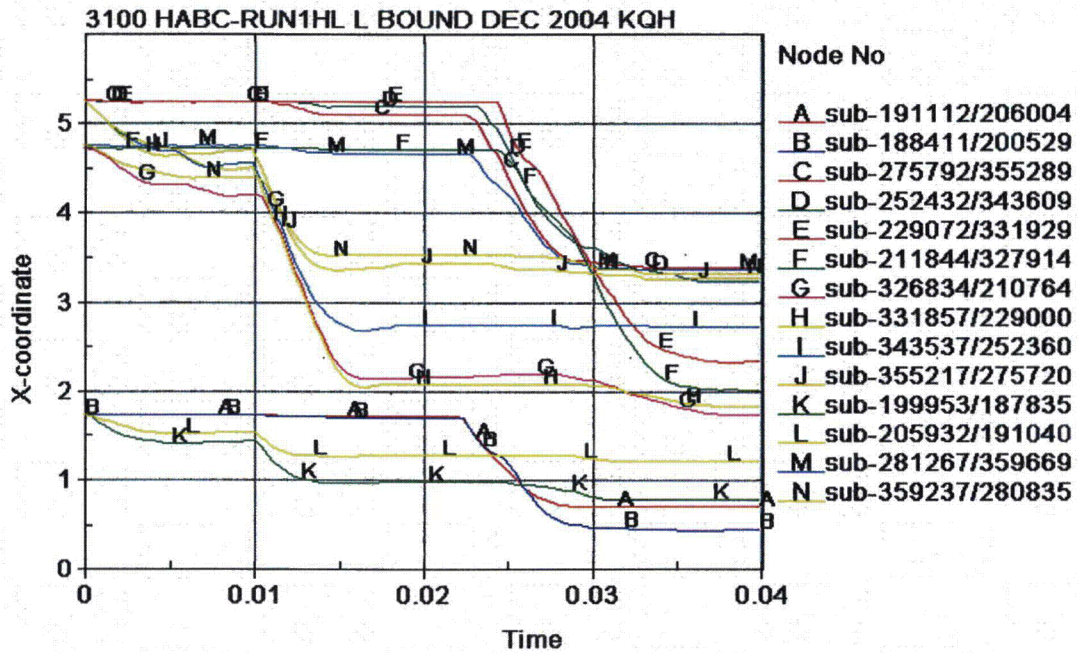


Figure 7.1.17 - HABC-run1hl, Kaolite Thickness Time History

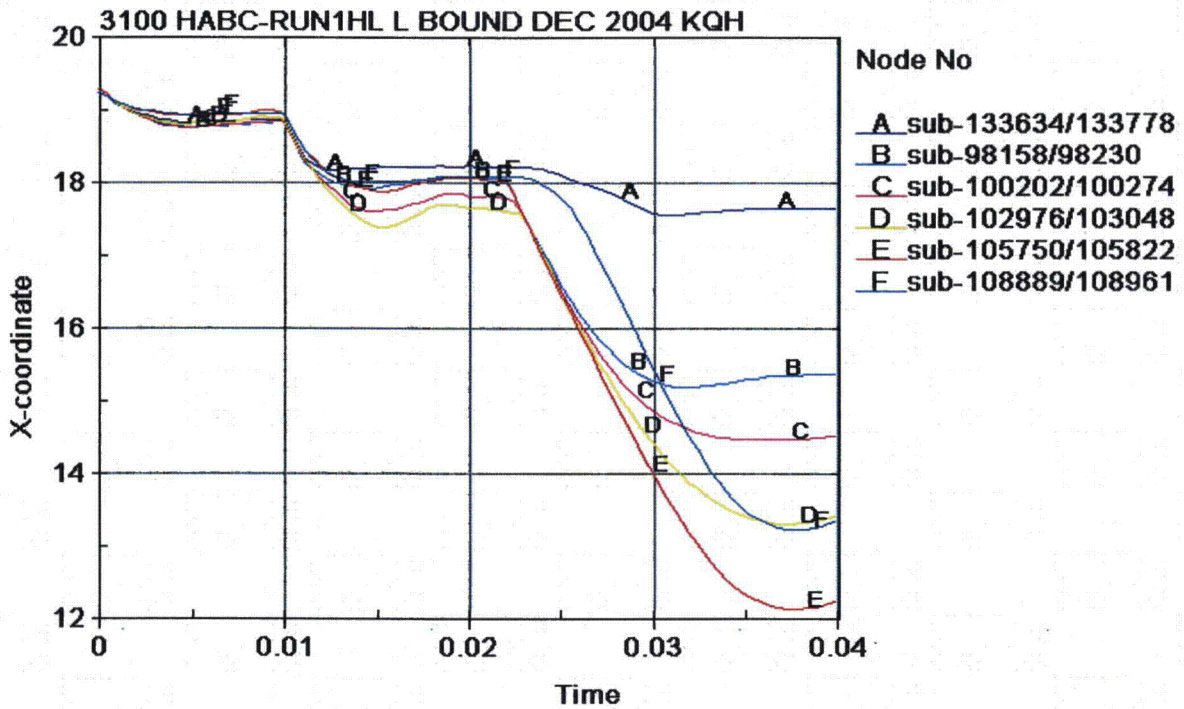


Figure 7.1.18 - HABC-run1hl, Drum Diameter Time History in the X Direction

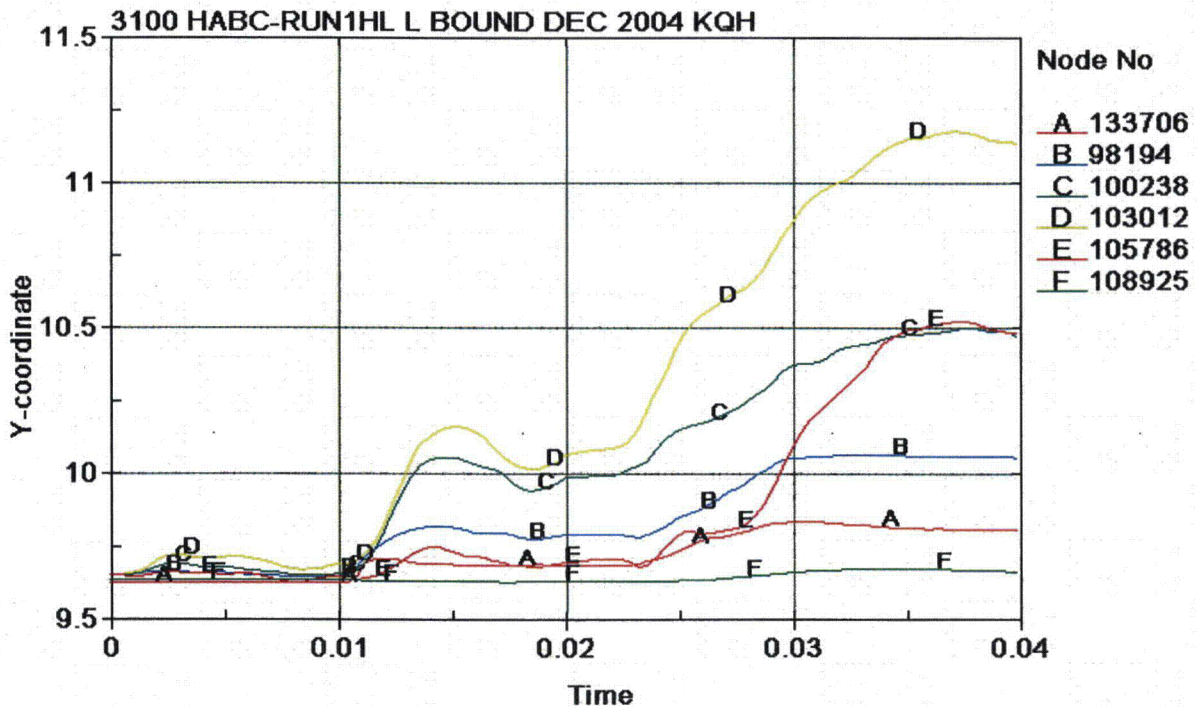


Figure 7.1.19 - HABC-run1hl, Drum Diameter Time History in the Y Direction

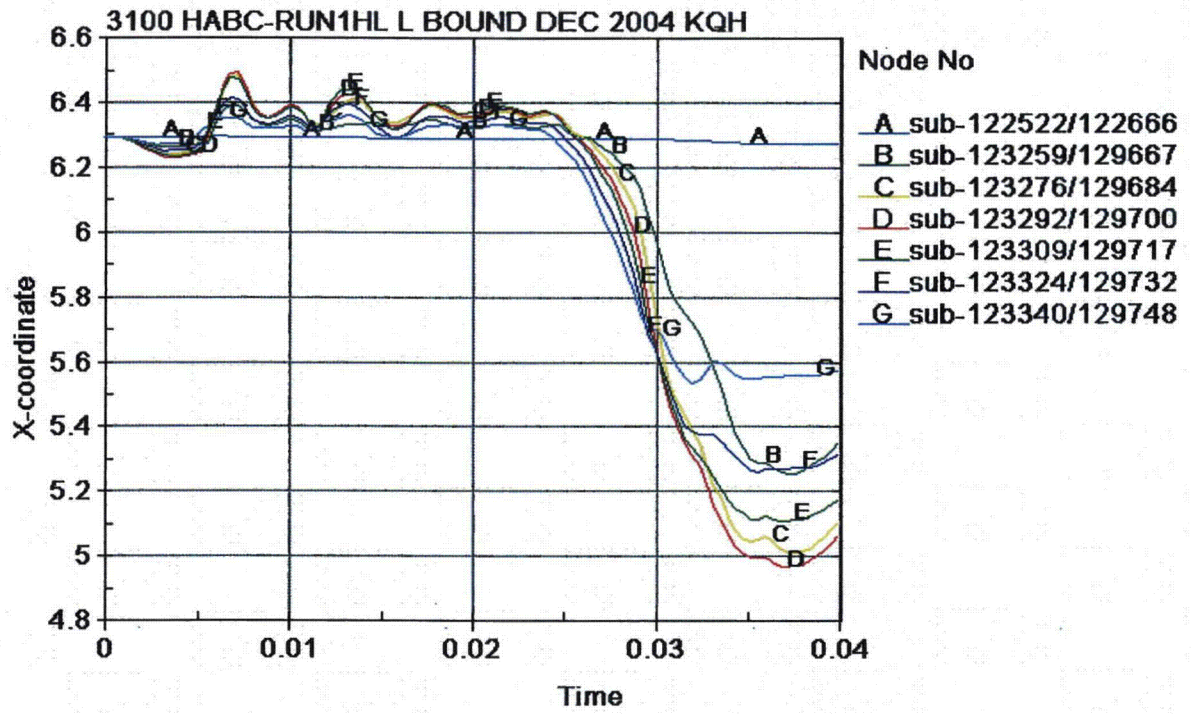


Figure 7.1.20 - HABC-run1hl, Diameter Changes in the Inner Liner

7.2 HABC-run1hh - Upper Bounding Side

HABC-run1hh are the runs with the lower bounding material properties for the kaolite and the HABC materials. The 4-foot impact occurs from time = 0.0 to 0.01 seconds; the 30-foot impact occurs from 0.01 to 0.0188 seconds; and the crush impact occurs from 0.0188 to 0.04 seconds.

The final configuration for the 4-foot impact is shown in Figure 7.2.1. The configuration at the ends of the package are shown in Figure 7.2.2. The effective plastic strain in the CV body for the 4-foot impact is shown in Figure 7.2.3 to be a maximum of 0.0238 in/in. The effective plastic strains in other package components for the 4-foot impact are listed in Table 7.2.1.

Component	Effective Plastic Strain, in/in
CV Lid	0.0000
CV Nut Ring	0.0000
Angle	0.0061
Drum	0.1207
Drum Bottom Head	0.1252
Liner	0.0991
Lid	0.1604
Lid Stiffener	0.0006
Lid Studs	0.0000
Lid Stud Nuts	0.0000
Lid Stud Washers	0.0411
Plug Liner	0.0045

The final configuration for the 30-foot impact is shown in Figure 7.2.4. The configuration at the ends of the package are shown in Figure 7.2.5. The maximum effective plastic strain for the 30-foot impact in the CV Body is 0.0347 in/in near the bottom head (Figure 7.2.6). The maximum effective plastic strain in the drum lid is 0.4063 in/in at the stud near the rigid plane as shown in Figure 7.2.7. The effective plastic strain in other components for the 30-foot impact are given in Table 7.2.2.

Table 7.2.2 - HABC-run1hh, 30-Foot Impact, Effective Plastic Strain Levels in Some Components	
Component	Effective Plastic Strain, in/in
CV Lid	0.0001
CV Nut Ring	0.0000
Angle	0.0632
Drum	0.2296
Drum Bottom Head	0.2517
Liner	0.1184
Lid Stiffener	0.0076
Lid Studs	0.1306
Lid Stud Nuts	0.0004
Lid Stud Washers	0.0424
Plug Liner	0.1072

The configuration after the crush impact is shown in Figure 7.2.8. The configuration at the ends of the package are shown in Figure 7.2.9. The maximum effective plastic strain for the crush impact in the CV body is 0.0525 in/in, on the crush plate side near the lid end of the top inner weight (Figure 7.2.10). The maximum effective plastic strain in the drum is 0.2814 in/in near the angle and the rigid plane (Figure 7.2.11). The maximum effective plastic strain in the drum lid is 0.6413 in/in (surface strain) as shown in Figure 7.2.12. The maximum occurs at the lid hole for the stud closest to the crush plate (180°). The membrane effective plastic strain is 0.4907 in/in at this location in the lid. Figure 7.2.13 shows that the maximum effective plastic strain in the studs is 0.2364 in/in. The effective plastic strain in other components are listed in Table 7.2.3 for the crush impact.

Table 7.2.3 - Run1hh, Crush Impact, Effective Plastic Strain Levels in Some Components	
Component	Effective Plastic Strain, in/in
CV Lid	0.0004
CV Nut Ring	0.0005
Angle	0.0845
Drum Bottom Head	0.2827
Liner	0.2022
Lid Stiffener	0.0171
Lid Stud Nuts	0.0018
Lid Stud Washers	0.0439
Plug Liner	0.1286

The lid separation time history is shown in Figure 7.2.14. The nodes are shown in Figure 3.1.30. The response is oscillatory with peak gap separation on the order of 0.010 in. At the end of the impact, the peaks are on the order of 0.006 in with an average gap on the order of 0.003 in or less.

The kaolite thickness time history is shown in Figure 7.2.15. The nodal pairs are shown in Figure 7.1.16.

Figure 7.2.16 and 7.2.17 show the drum diameter and radial time histories. The nodes are defined in Figure 3.1.34.

Figure 7.2.18 shows the diameter response of the liner. Figure 3.1.37 and Table 3.1.3 define the liner nodes used in Figure 7.2.18.

3100 HABC-RUN1HH U BOUND DEC 2004 KQH
Time = 0.0099999

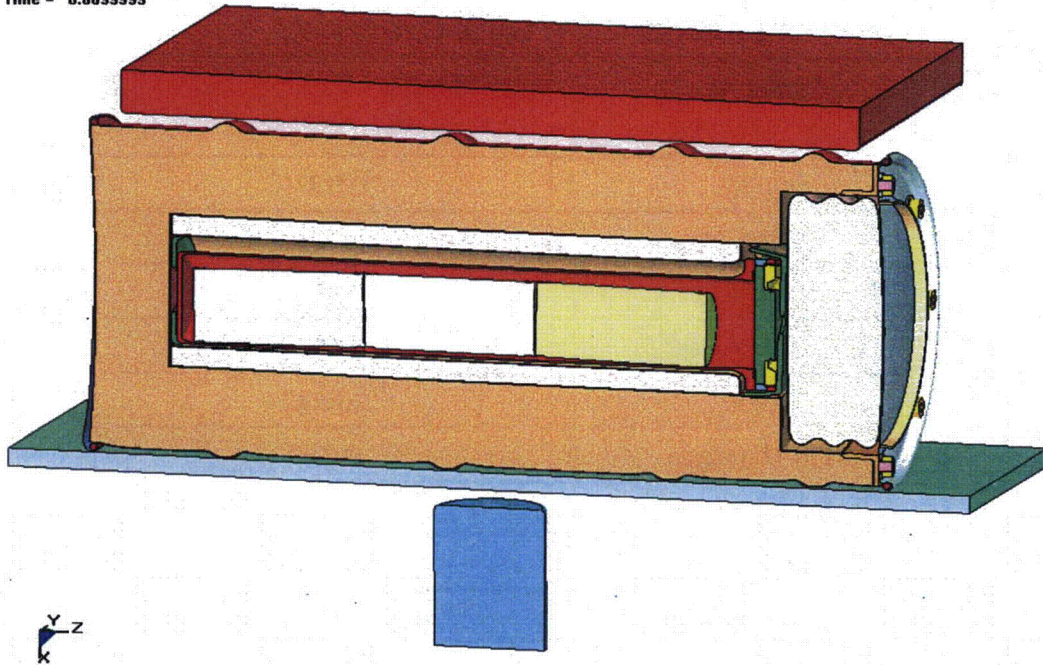


Figure 7.2.1 - HABC-run1hh, Configuration After the 4-Foot Impact

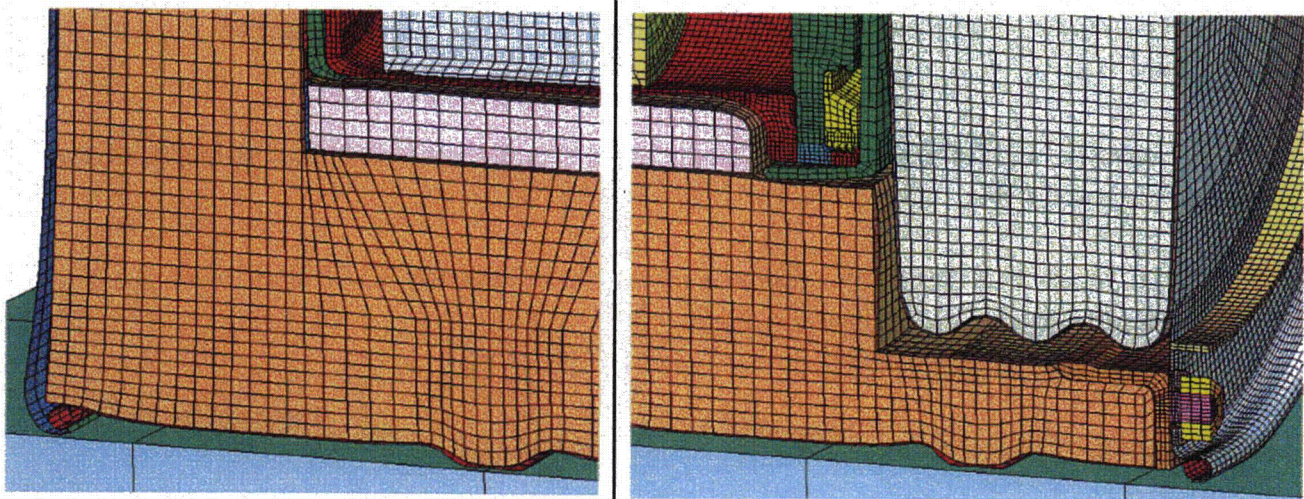


Figure 7.2.2 - HABC-run1hh, 4-Foot Impact, Configuration of the Lid and Bottom

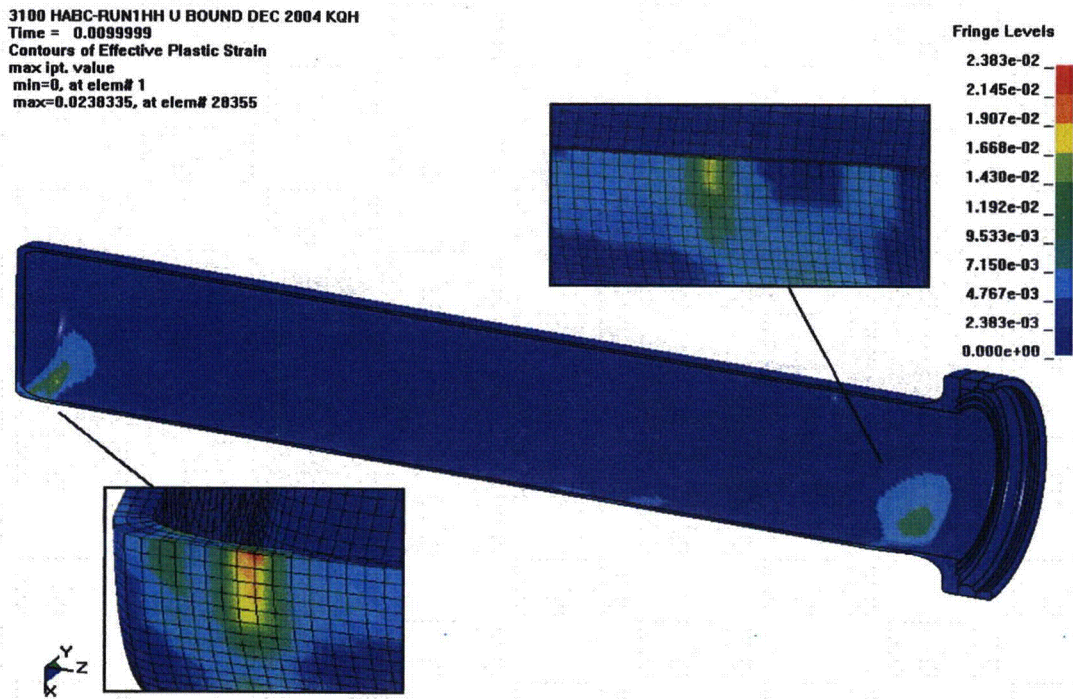


Figure 7.2.3 - HABC-run1hh, 4-Foot Impact, Effective Plastic Strain in the CV Body

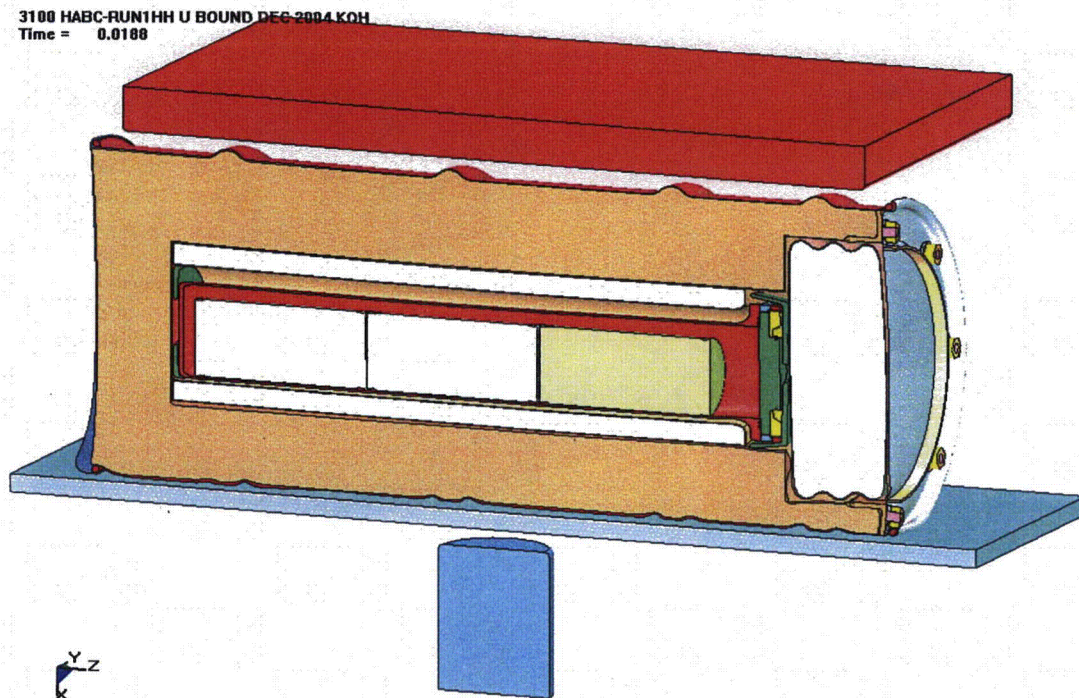


Figure 7.2.4 - HABC-run1hh, Configuration After the 30-Foot Impact

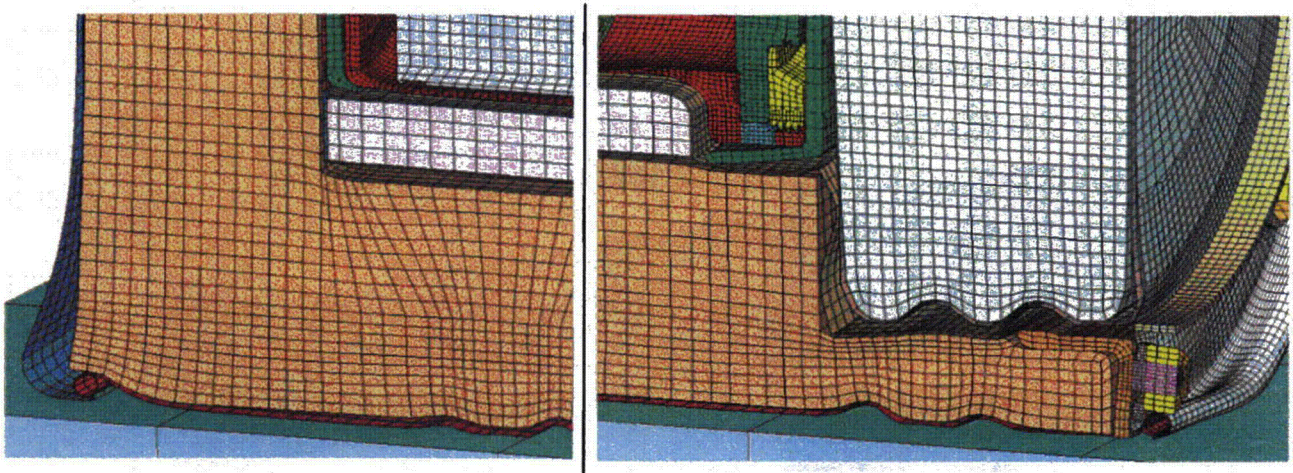


Figure 7.2.5 - HABC-run1hh, 30-Foot Impact, Configuration of the Lid and Bottom

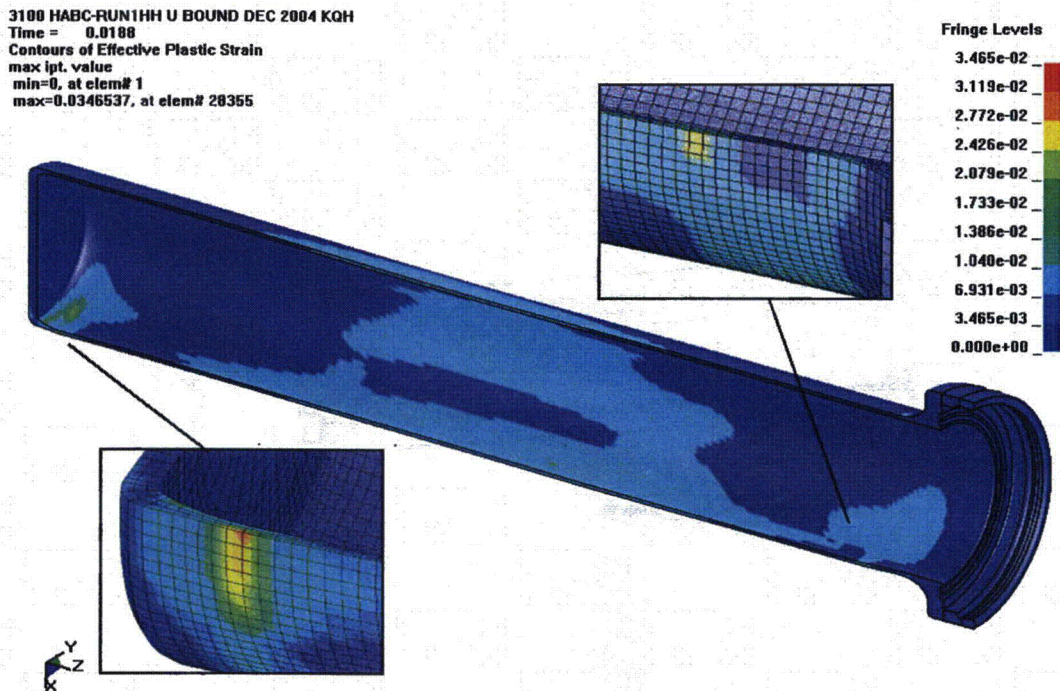


Figure 7.2.6 - HABC-run1hh,30-Foot Impact, Effective Plastic Strain in the CV Body

3100 HABC-RUN1HH U BOUND DEC 2004 KQH
Time = 0.0188
Contours of Effective Plastic Strain
max ipt. value
min=0, at elem# 37788
max=0.40629, at elem# 37701

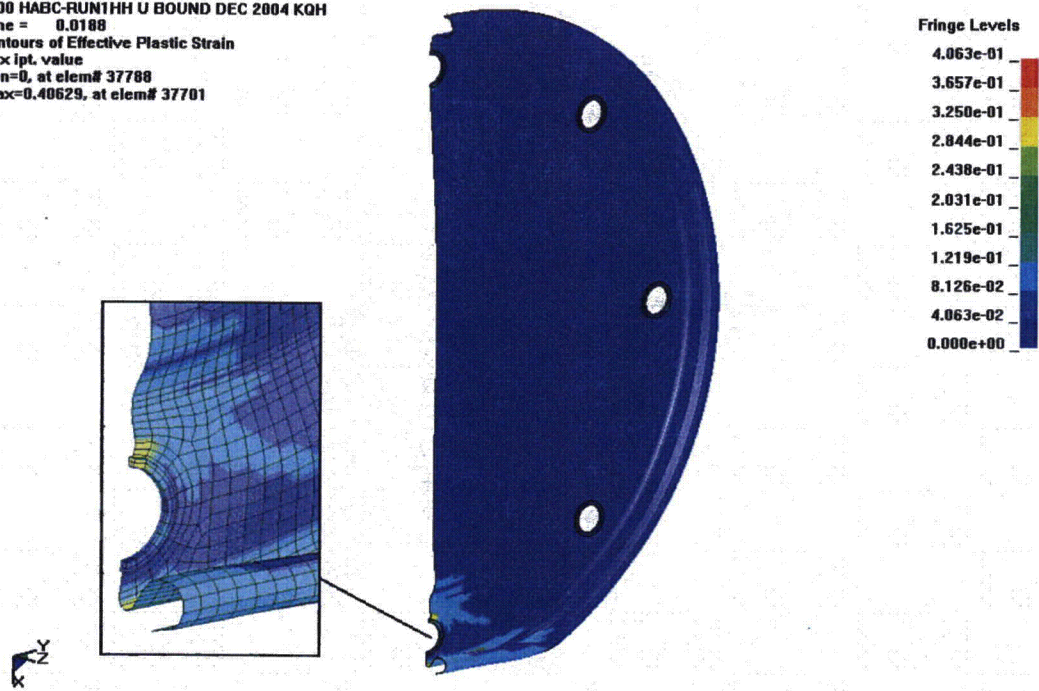


Figure 7.2.7 - HABC-run1hh, 30-Foot Impact, Effective Plastic Strain in the Lid

3100 HABC-RUN1HH U BOUND DEC 2004 KQH
Time = 0.04

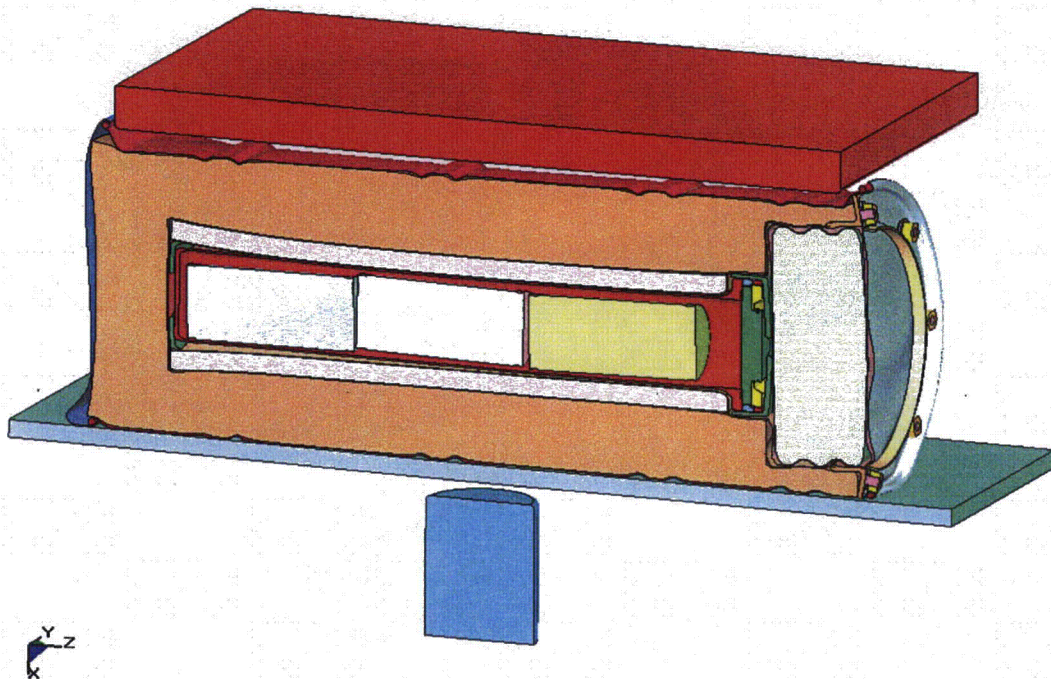


Figure 7.2.8 - HABC-run1hh, Configuration After the Crush Impact

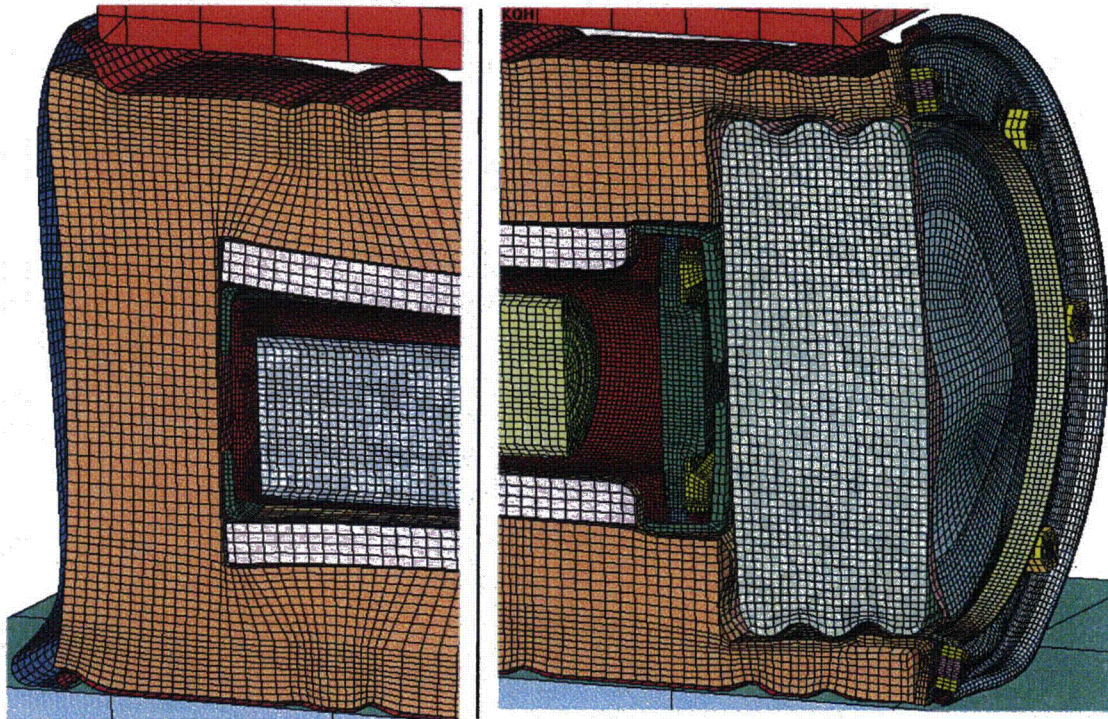


Figure 7.2.9 - HABC-run1hh, Crush Impact, Configuration of the Lid and Bottom

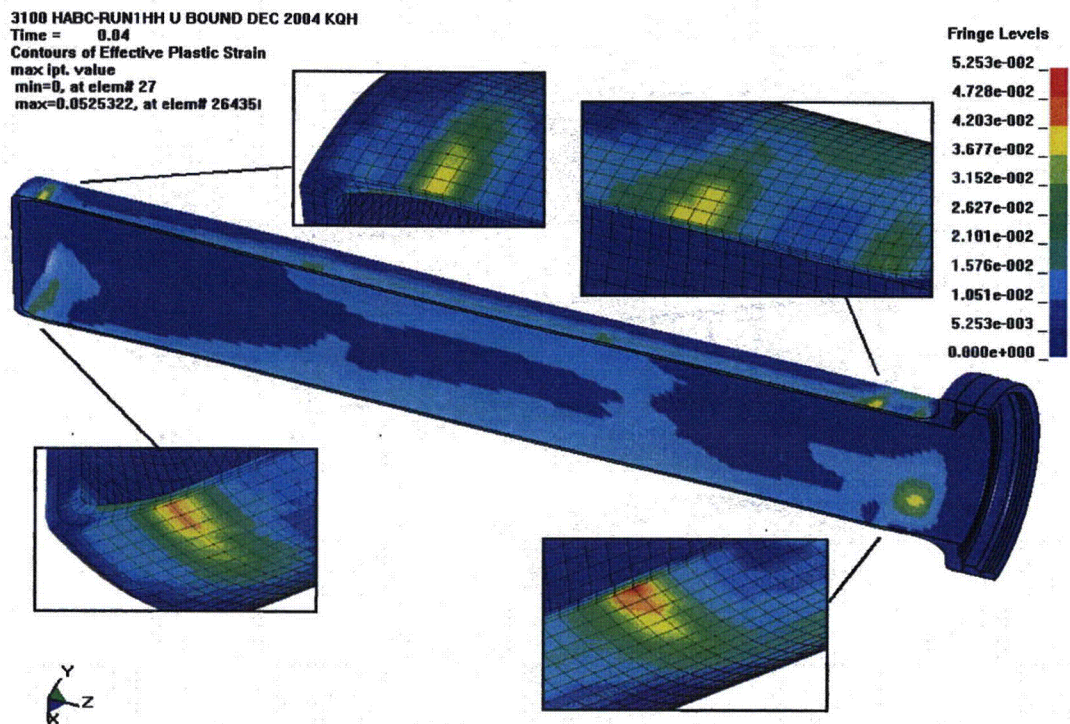


Figure 7.2.10 - HABC-run1hh, Crush Impact, Effective Plastic Strain in the CV Body

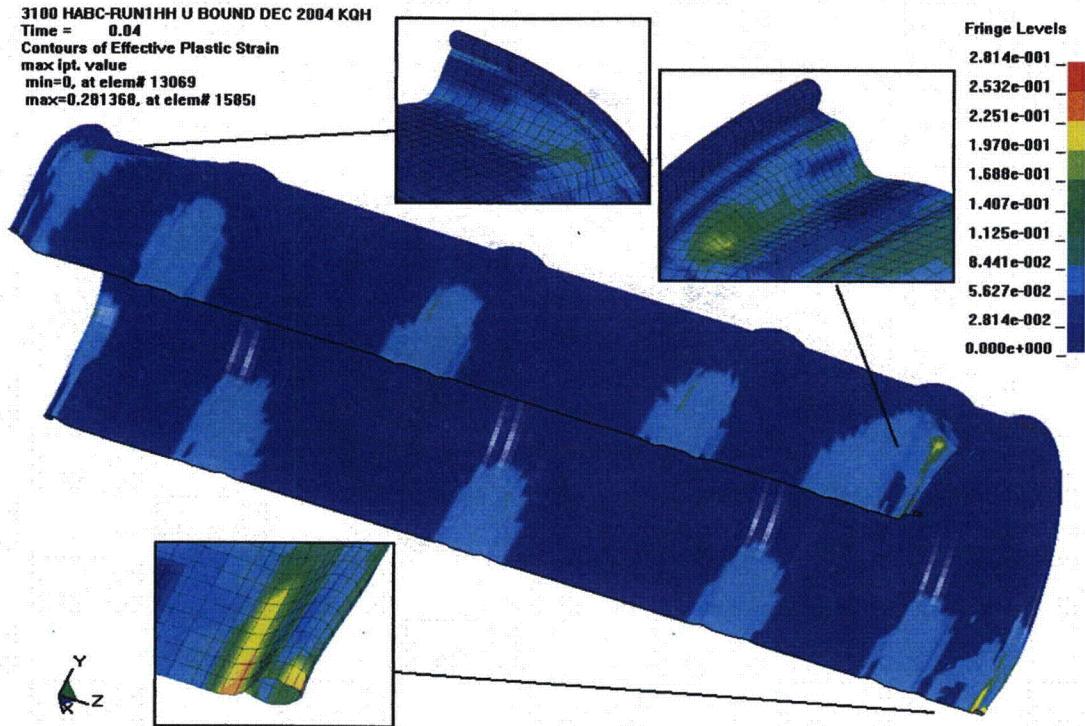


Figure 7.2.11 - HABC-run1hh, Crush Impact, Effective Plastic Strain in the Drum

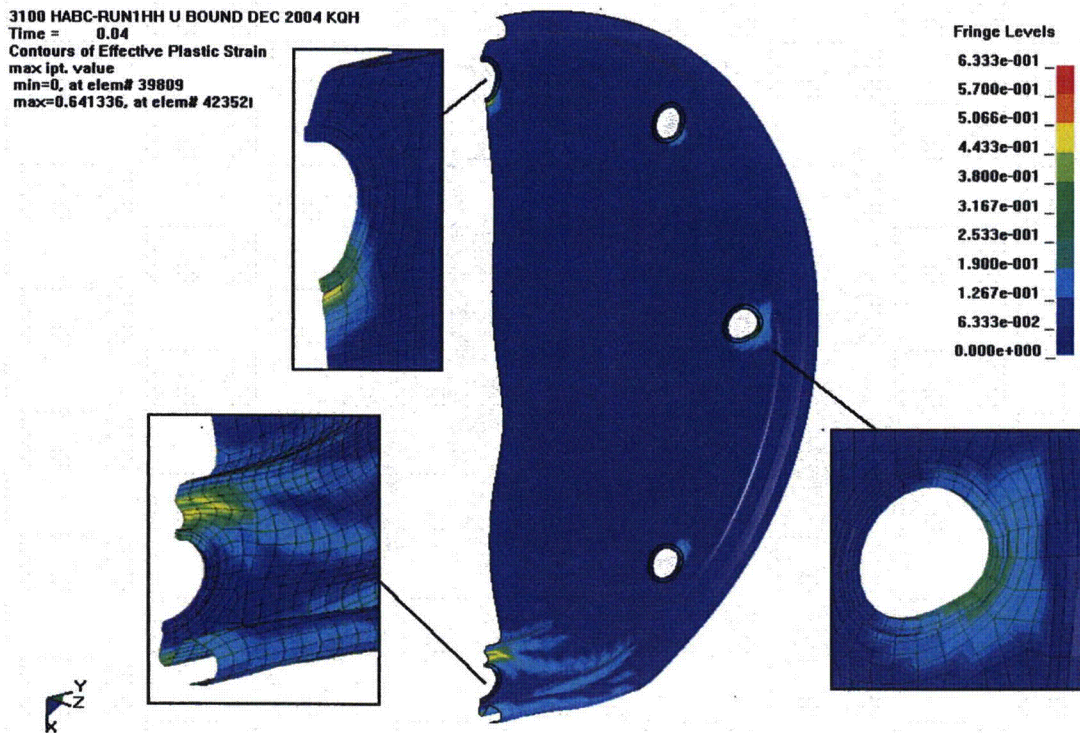


Figure 7.2.12 - HABC-run1hh, Crush Impact, Effective Plastic Strain in the Lid

3100 HABC-RUN1HH U BOUND DEC 2004 KQH
 Time = 0.04
 Contours of Effective Plastic Strain
 max ipt. value
 min=0, at elem# 71878
 max=0.236427, at elem# 719921

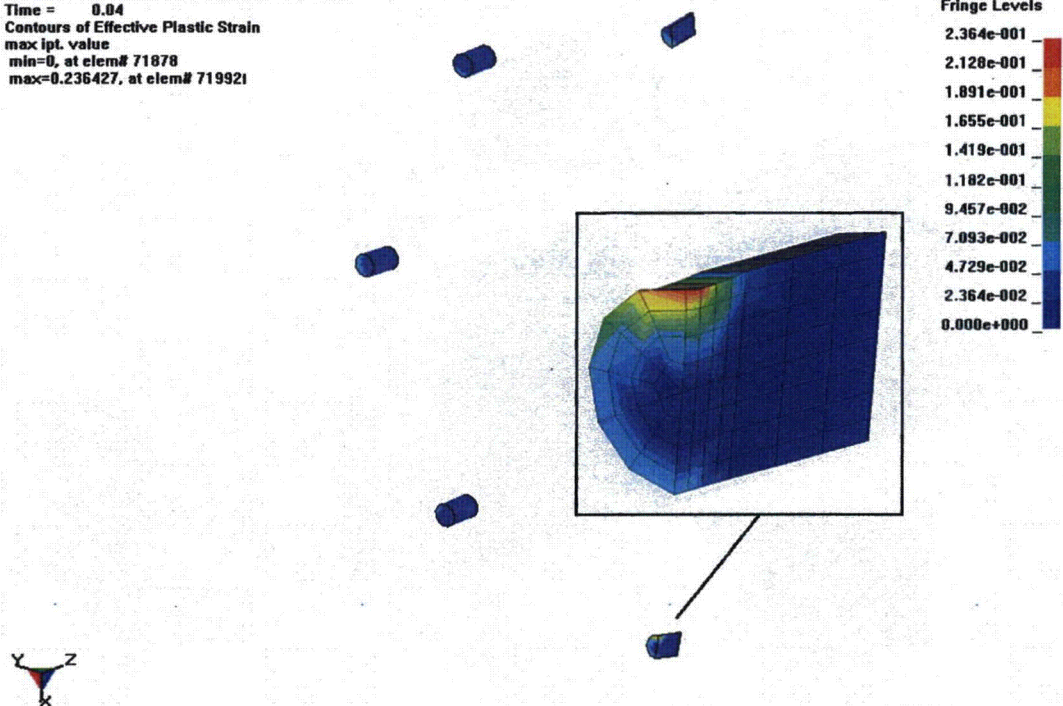


Figure 7.2.13 - HABC-run1hh, Crush Impact, Effective Plastic Strain in the Studs

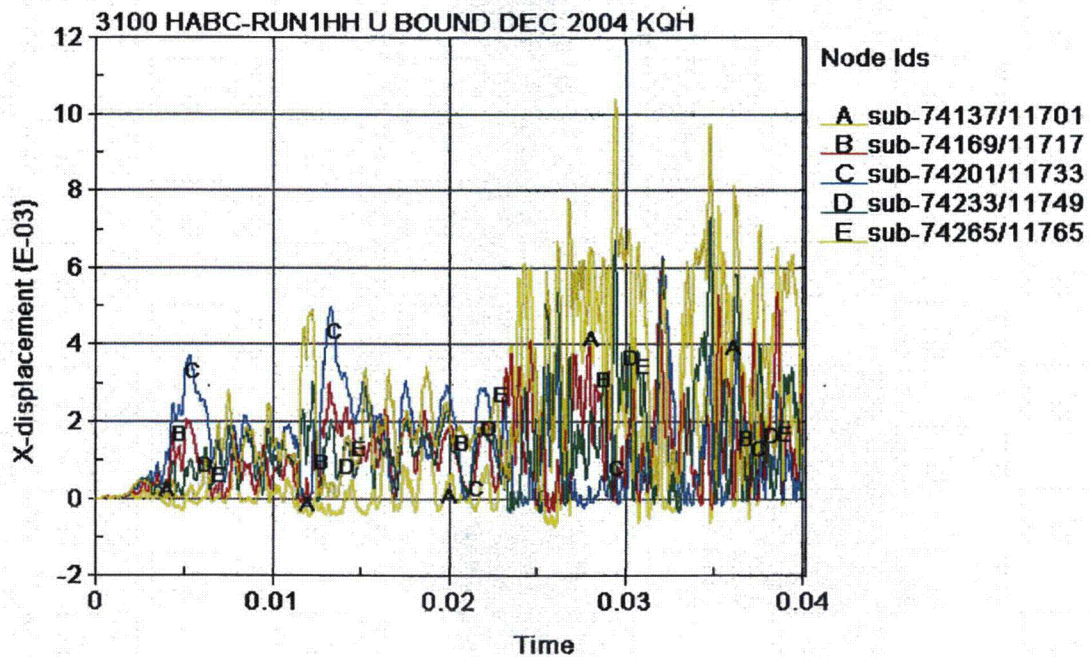


Figure 7.2.14 - HABC-run1hh, CV Lid Separation Time History

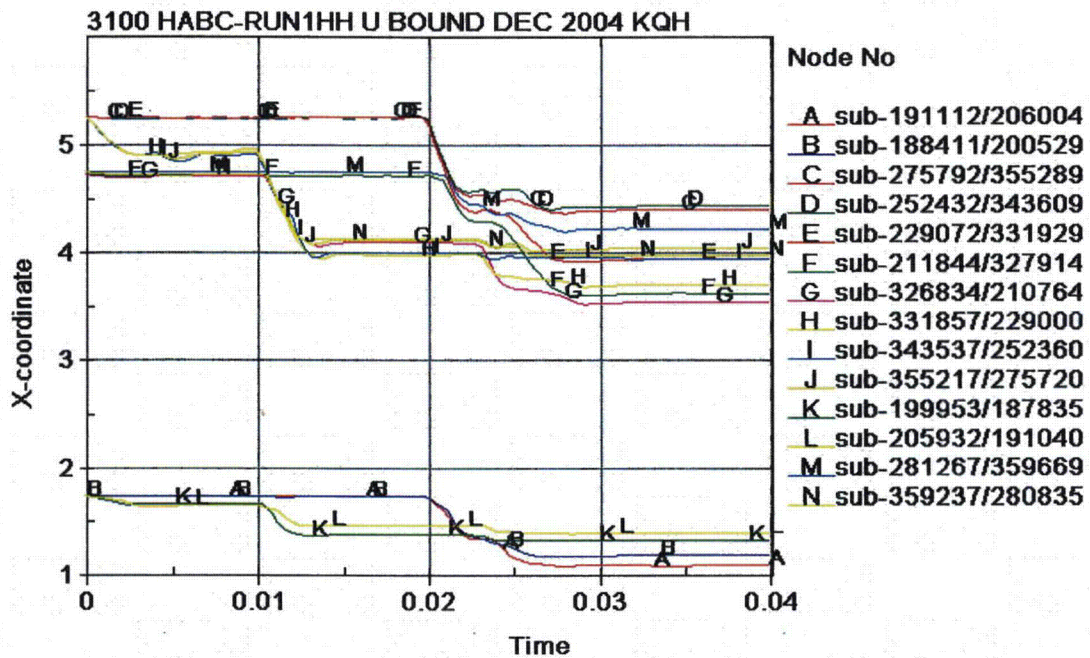


Figure 7.2.15 - HABC-run1hh, Kaolite Thickness Time History

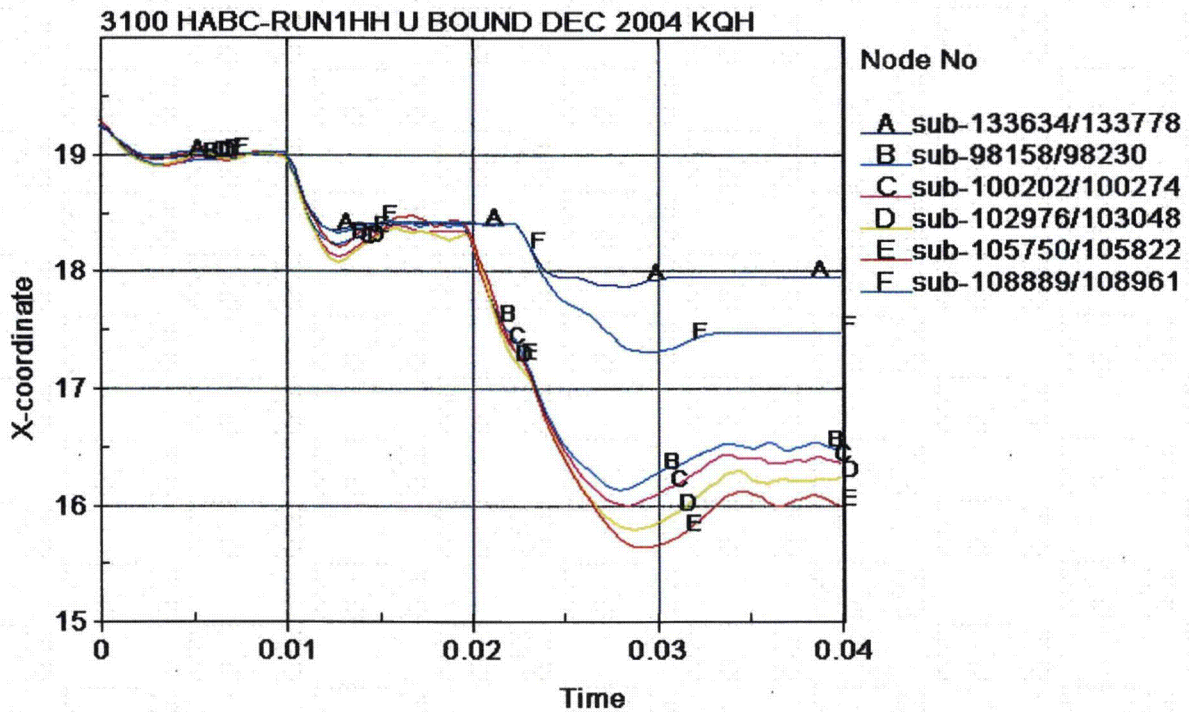


Figure 7.2.16 - HABC-run1hh, Drum Diameter Time History in the X Direction

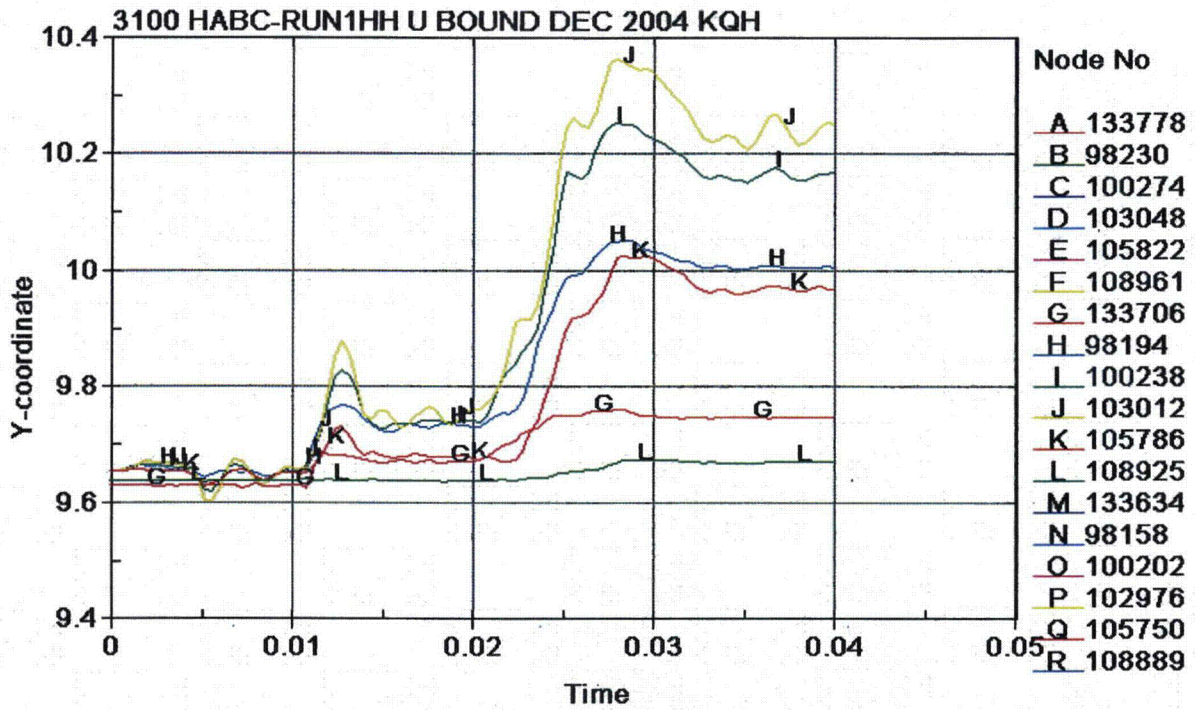


Figure 7.2.17 - HABC-run1hh, Drum Diameter Time History in the Y Direction

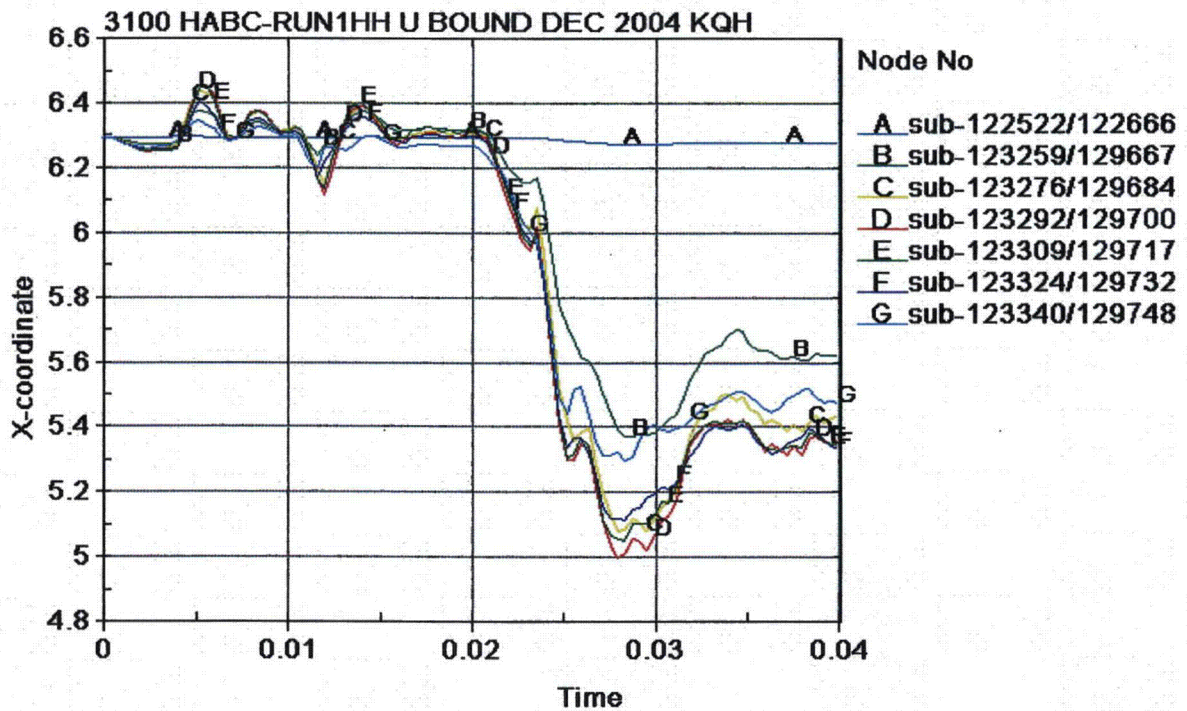


Figure 7.2.18 - HABC-run1hh, Diameter Changes in the Inner Liner